Immunology and Inflammation

CXXC-finger protein 1 associates with FOXP3 to stabilize homeostasis and suppressive functions of regulatory T cells

Xiaoyu Meng, Yezhang Zhu, Kuai Liu, Yuxi Wang, Xiaoqian Liu, Chenxin Liu, Yan Zeng, Shuai Wang, Xianzhi Gao, Xin Shen, Jing Chen, Sijue Tao, Qianying Xu, Linjia Dong, Li Shen, Lie Wang

Institute of Immunology and Bone Marrow Transplantation Center, The First Affiliated Hospital, Zhejiang University School of Medicine, Hangzhou, China • Zhejiang University School of Medicine, Hangzhou, China • Liangzhu Laboratory, Zhejiang University Medical Center, Hangzhou, China • Department of Hematology, Tongji Hospital, School of Medicine, Tongji University, Shanghai, China • Shanghai Key Laboratory of Signaling and Disease Research, Frontier Science Center of Stem Cell Research, National Stem Cell Translational Resource Center, School of Life Sciences and Technology, Tongji University, Shanghai, China • Laboratory Animal Center, Zhejiang University, Hangzhou, China • Co-Facility Center, Zhejiang University School of Medicine, Hangzhou, China • Department of Gastrointestinal Surgery, The Second Affiliated Hospital, Zhejiang University School of Medicine, Hangzhou, China • School of Basic Medical Sciences and Forensic Medicine, Hangzhou Medical College, Hangzhou, China • MOE Key Laboratory of Biosystems Homeostasis & Protection and Zhejiang Provincial Key Laboratory for Cancer Molecular Cell Biology, Life Sciences Institute, Zhejiang University, Hangzhou, China • Department of Orthopedics Surgery, the Second Affiliated Hospital, School of Medicine, Zhejiang University, Hangzhou, China • Future Health Laboratory, Innovation Center of Yangtze River Delta, Zhejiang University, Jiaxing, China

A newer version is available. **Read the latest version**.

Version of Record
April 4, 2025

Reviewed Preprint
v2 • March 19, 2025
Revised by authors

Reviewed Preprint
v1 • November 21, 2024

eLife Assessment

This study presents **important** findings on the role of CXXC-finger protein 1 in regulatory T cell gene regulation and function. The evidence supporting the authors' claims is **convincing**, with mostly state-of-the-art technology. The work will be of relevance to immunologists interested in regulatory T cell biology and autoimmunity.

https://doi.org/10.7554/eLife.103417.2.sa4

Abstract

FOXP3-expressing regulatory T (T_{reg}) cells play a pivotal role in maintaining immune homeostasis and tolerance, with their activation being crucial for preventing various inflammatory responses. However, the mechanisms governing the epigenetic program in T_{reg} cells during their dynamic activation remain unclear. In this study, we demonstrate that CXXC finger protein 1 (CXXC1) interacts with the transcription factor FOXP3 and facilitates the regulation of target genes by modulating H3K4me3 deposition. *Cxxc1* deletion in T_{reg} cells leads to severe inflammatory disease and spontaneous T-cell activation, with impaired

immunosuppressive function. As a transcriptional regulator, CXXC1 promotes the expression of key T_{reg} functional markers under steady-state conditions, which are essential for the maintenance of T_{reg} cell homeostasis and their suppressive functions. Epigenetically, CXXC1 binds to the genomic regulatory regions of T_{reg} program genes in mouse T_{reg} cells, overlapping with FOXP3 binding sites. Given its critical role in T_{reg} cell homeostasis, CXXC1 presents itself as a promising therapeutic target for autoimmune diseases.

Introduction

Regulatory T (T_{reg}) cells are a distinct subset of $CD4^+$ T cells that play a critical role in maintaining immune homeostasis and self-tolerance by suppressing excessive or aberrant immune responses to foreign or self-antigens [1–3]. These cells can be further categorized into thymus-derived regulatory T cells (tT_{reg} cells), periphery-derived T_{reg} cells (pT_{reg} cells), and induced T_{reg} cells (iT_{reg} cells) [4]. They uniquely express the transcription factor FOXP3, a member of the forkhead winged-helix family, which is essential for T_{reg} cell lineage commitment and suppressive function [5,6]. Deletion or mutation of the *Foxp3* gene leads to a range of immunological disorders, including allergies, immunopathology, and autoimmune diseases in both mice and humans [7,8].

It is well established that FOXP3 recruits various cofactors to form complexes that either promote or repress the expression of downstream genes, with histone and DNA modifications playing pivotal roles in this process. FOXP3 can activate or repress the transcription of key regulators of T_{reg} cell activation and function by recruiting the histone acetyltransferases (HATs) or histone deacetylases (HDACs)[9,10]. Notably, FOXP3-bound sites exhibit enrichment of H3K27me3, a modification essential for FOXP3-mediated repressive chromatin remodeling under inflammatory conditions[11]. However, the direct role of FOXP3 as a transcriptional activator through interactions with epigenetic regulators, particularly via modulation of H3K4 trimethylation, remains poorly documented.

In mammals, six proteins have been identified that catalyze H3K4 methylation. These proteins contain the SET domain and include MLL1 (KMT2A), MLL2 (KMT2B), MLL3 (KMT2C), MLL4 (KMT2D), SETD1A, and SETD1B [12,13]. For example, MLL1 plays a critical role as an epigenetic regulator in T_{reg} cell activation and functional specialization[14]. Additionally, Placek *et al.* demonstrated that MLL4 is essential for T_{reg} cell development by catalyzing H3K4me1 at distant unbound enhancers through chromatin looping [15]. H3K4me3, which is enriched at the transcription start site (TSS) and the CpG island (CGI), converts chromatin into active euchromatin by recruiting activating factors [16]. CXXC finger protein 1(CXXC1, also known as CFP1), which contains a SET1 interaction domain (SID), is required for binding to the histone H3K4 methyltransferases SETD1A and SETD1B [17]. Previous studies have shown that CXXC1 regulates promoter patterns during T cell maturation, GM-CSF-derived macrophage phagocytosis, TH17 cell differentiation, and the function of ILC3 cells with aging by modulating H3K4me3 modification[18–21]. Despite the well-documented role of CXXC1 in various immune effector cells, its role in T_{reg} cells remains unclear.

Here, we demonstrate that CXXC1 interacts with FOXP3 and enhances the expression of FOXP3 target genes. T_{reg} cell-specific deletion of *Cxxc1* triggers systemic autoimmunity, accompanied by multiorgan inflammation, ultimately resulting in early-onset fatal inflammatory disease in mice. *Cxxc1*-deficient T_{reg} cells exhibit a disadvantage in proliferation and homeostasis, even in non-inflammatory mice where coexisting wild-type (WT) T_{reg} cells were present. Moreover, *Cxxc1*-deficient T_{reg} cells display intrinsic defects in the expression of key suppression molecules, including CTLA-4, CD25, ICOS, and GITR. Consistent with these findings, mechanistic studies strongly suggest that CXXC1 functions as an essential cofactor of FOXP3, playing a crucial role in sustaining H3K4me3 modifications at key T_{reg} cell genes.

Materials and Methods

Mice

All mice used in this study were bred for a minimum of seven generations on a C57BL/6 background. Mouse experiments, or cells from mice of the same genotype, compared littermates or age-matched control animals. The *Cxxc1*$^{fl/fl}$ mouse strain has been previously described [22]. The *Foxp3*^{cre} mice (JAX,016959) were generously provided by Bin Li (Shanghai Jiao Tong University School of Medicine, Shanghai, China). CD45.1 (NM-KI-210226) mice were purchased from the Nanjing Biomedical Research Institute of Nanjing University. *Rag1*$^{-/-}$mice (stock#T004753) were purchased from GemPharmatech. 2D2 (MOG35-55-specific TCR transgenic) mice were graciously supplied by Prof. Linrong Lu (Zhejiang University School of Medicine, Hangzhou, Zhejiang, China). *Foxp3*^{cre} (WT) and *Foxp3*^{cre} *Cxxc1*$^{fl/fl}$ (cKO) were utilized at 3 weeks old unless otherwise stated. All mice were housed in the Zhejiang University Laboratory Animal Center under specific pathogen-free conditions, and all animal experimental procedures were approved by the Zhejiang University Animal Care and Use Committee (approval no.ZJU20230246).

Cell culture

HEK 293T cells were obtained from ATCC, and Plat E cells were kindly provided by Prof. Xiaolong Liu (Shanghai Institutes for Biological Sciences). Both cell lines were cultured in Dulbecco-modified Eagle medium (DMEM) containing 10% (v/v) fetal bovine serum (FBS), supplemented with 1% penicillin/streptomycin.

Immunofluorescence (IF) Staining

As previously described [23], coverslips were treated with a 0.01% poly-L-lysine solution (P4707; Sigma) for 10 minutes, air-dried, and then coated with $CD4^+$ YFP^+ T_{reg} cells. The cells were then fixed in 4% formaldehyde for 15 minutes at room temperature, permeabilized with 0.2% Triton X-100, and blocked with 1% BSA. Antibodies against CXXC1 (ab198977; Abcam) and FOXP3(17-5773-82; Invitrogen) were diluted in Image iT FX signal enhancer (I3693; Invitrogen) and incubated with cells overnight at 4 °C. After washing with phosphate-buffered saline (PBS), the cells were incubated with a goat anti-rabbit antibody Alexa Fluor 594 (1:250;10015289; Invitrogen) secondary antibody and stained with DAPI (200 ng/mL; D523; Dojindo). Slides were washed with PBS and sealed with an antifade solution(P36934; Invitrogen) before imaging with an Olympus FV3000 fluorescence microscope. The images were visualized using the FV31-SW software.

Co-immunoprecipitation and western blot

Harvest the appropriate transfected cell lines and primary cells from culture and wash them with ice-cold PBS. Lyse the cells in NETN300 buffer (300CmM NaCl, 0.5CmM EDTA, 0.5% (v/v) NP-40, 20CmM Tris-HCl pH 8.0) supplemented with a protease inhibitor (1:100, P8340, Sigma-Aldrich) and PMSF (1 mM) on ice for 10 minutes. Take a small portion of the whole-cell lysate as input, and incubate the remaining lysate with either Anti-FLAG M2 Beads (M8823; Sigma) or Anti-HA Beads (HY-K0201; MCE) on a rotator at 4°C overnight. For the endogenous Co-IP assay targeting CXXC1 and FOXP3, incubate the cell lysate with protein G magnetic beads along with anti-CXXC1 (ab198977; Abcam) or anti-FOXP3 (14-4774-82; Invitrogen) antibodies on a rotator at 4°C overnight. Wash the beads three times with IP buffer (100CmM NaCl, 0.5CmM EDTA, 0.5% (v/v) NP-40, 20CmM Tris-HCl pH 8.0) to remove non-specific binding. Boil the washed beads with 1× Laemmli sample buffer (1610747; Bio-Rad) to elute the bound proteins. Separate the denatured proteins by SDS-PAGE. Transfer the separated proteins onto PVDF membranes (Millipore) for immunoblotting.Immunoblot the PVDF membranes (IPVH00010) with the following antibodies: anti-CXXC1 (1:1000; ab198977; Abcam), anti-FOXP3 (1:500; 14-7979-80; Invitrogen), anti-FlAG

(1:1000; 14793; Cell Signaling Technology), anti-HA (1:1000; 3724S; Cell Signaling Technology).Detect the immunoblotted proteins using a secondary HRP-conjugated goat anti-rabbit antibody (1:1000; HA1001-100; Huabio) and visualize the bands using an appropriate detection method.

ELISA

Serum samples from 3-week-old WT and KO mice were analyzed for total IgG and IgE concentrations using ELISA kits (88-50630-88; eBioscience) according to the manufacturer's instructions. Half-area ELISA plates were coated with Coating Buffer and incubated overnight at 4°C. After washing with PBST (PBS, 1 mM EDTA, 0.05% Tween-20), the plates were blocked with 5% BSA in PBS for 30 minutes at room temperature. Serum was diluted to the appropriate concentration with blocking buffer and incubated overnight at 4°C. After washing with PBST, the plates were incubated with HRP-conjugated anti-mouse IgG(1033-05; SouthernBiotech) and IgE(1110-05; SouthernBiotech) antibodies (1:2000 in 1% BSA/PBST) at 37°C for 1 hour. Following washing, TMB substrate was added, and the reaction was stopped with 2 M HCSOC after sufficient color development (1–15 minutes). Absorbance at 450 nm was measured within 30 minutes.

Lymphocyte Isolation and Flow Cytometry

Cells from lymphoid organs were prepared by mechanical disruption between frosted slides, while non-lymphoid organs were processed enzymatically. For lung tissue, minced samples were digested in RPMI containing 100 μg/mL DNase I (9003-98-9;Sigma-Aldrich) and 2 mg/mL Collagenase D (LS004188;Worthington Biochemical) at 37°C for 1.5 hours. Liver tissue was minced and digested in RPMI supplemented with 100 μg/mL DNase I and 1 mg/mL Collagenase D at 37°C for 30 minutes, with lymphocytes isolated using a 40-70% Percoll (GE Healthcare) gradient. For intestinal tissue, the samples were first incubated in DMEM containing 3% FBS, 0.2% HEPES, 0.5 M EDTA, and 0.145 mg/mL dithiothreitol for 10 minutes. This was followed by digestion with 50 mg/mL DNase I and 145 mg/mL Collagenase II (Worthington Biochemical) in DMEM at 37°C for 5 minutes. Lymphocytes were then isolated using an 80% and 40% Percoll gradient.

For surface marker analysis, cells were incubated for 15 minutes with purified anti-mouse CD16/32 antibody (101320; BioLegend) to block Fc receptors. After blocking, cells were stained with the indicated antibodies for surface markers. To determine cytokine expression, cells were stimulated for 4 hours at 37C with phorbol12-myristate13-acetate (50ng/mL; S1819; Beyotime), ionomycin (1mg/ml; S1672; Beyotime), and brefeldin A (BFA;00-4506-51; Invitrogen). After stimulation, cells were labeled with a fixable viability dye and surface markers. Cells were then fixed and permeabilized according to the manufacturer's instructions (00-8222-49; Invitrogen). For transcription factor staining, samples were fixed using the FOXP3/Transcription Factor Staining Buffer Set (00-5523-00; Invitrogen). Flow cytometry was conducted using a BD Fortessa (BD Biosciences) or LongCyte (Beijing Challen Biotechnology Co., Ltd.) system. Flow cytometry data were acquired and analyzed using FlowJo software.

The following antibodies were purchased from Invitrogen or BioLegend: Zombie Viole t f-ixable viability(423113), Zombie NIR fixable(423105), CD25(PC61), CD8α(53-6.7), CD62L(MEL-14), PD-1(J43), CD44(IM7), IL-17A(TC1118H10), KL-RG1(2F1), CD4 (GK1.5), TCRβ(H57-597), IFN-γ(XMG1.2), FOXP3(FJK-16s), CTLA-4(UC10-4B9), IC OS(15F9), GITR(DTA-1), LAG3(C9B7W), TCRVβ11(RR3-15), CD45RB(C363-16A) C D69 (H1.2F3), MHCII(M5/114.15.2), CD80(16-10A1), T-bet(eBio4B10), IKZF4(ESB7C 2), IL-4(11B11), CCR7(4B12), CD73(TY/11.8).

Real-time PCR

Total RNA was extracted from T_{reg} cells using the RNAAiso Plus(9109; Takara) reagent according to the manufacturer's instructions, and cDNA synthesis was performed using the Prime Script RT Reagent Kit (Takara). TB Green Premix Ex Taq (RR420A; Takara) was used for quantitative real-

time PCR (qPCR). The expression levels of target mRNA were normalized to the level of β-*actin* expression. The primers for qPCR are as follows:

- *Cxxc1* qPCR Forward: ATCCGGGAATGGTACTGTCG
- *Cxxc1* qPCR Reverse: CTGTGGAGAAGATTTGTGGG
- *β-actin* qPCR Forward: CTGTCCCTGTATGCCTCTG
- *β-actin* qPCR Reverse: ATGTCACGCACGATTTCC

$CD4^+$T and YFP^+ T_{reg} cells adoptive transfer in Experimental autoimmune encephalomyelitis (EAE)

$CD4^+YFP^+$ T_{reg} cells from *Foxp3*^{cre} and *Foxp3*^{cre} *Cxxc1*$^{fl/fl}$ mice were enriched using the Mouse CD4 T Cell Isolation Kit (480005; Biolegend) and then sorted using the BD Aria II flow cytometer. Naïve $CD4^+$T cells from 2D2 (MOG35-55-specificTCR transgenic) mice were isolated using the Mouse CD4 Naïve T cell Isolation Kit480039 (480039; Biolegend). As previously described[24], 2D2 naïve $CD4^+$ T cells alone (5×10^5 per mouse), or 2D2 naïve $CD4^+$ T cells (5×10^5 per mouse) together with WT or *Foxp3*^{cre}*Cxxc1*$^{fl/fl}$ T_{reg} cells (2×10^5 per mouse), were transferred into *Rag1*$^{-/-}$ mice via the tail vein. One day after cell transfer, the recipient mice were inoculated subcutaneously (s.c.) with 200μg MOG35-55 peptide (MEVGWYRSPFSRVVHLYRNGK; GenemeSynthesis) emulsified in complete Freund's adjuvant (CFA) (F5506; Sigma). Intravenous administration of 200 ng of Pertussis toxin (181; List Biological Laboratories) was performed on days 0 and 2 after peptide inoculation. The severity of EAE was monitored and blindly graded using a clinical score from 0 to 5: 0, no clinical signs; 1, limp tail; 2, paraparesis (weakness, incomplete paralysis of one or two hind limbs); 3, paraplegia (complete paralysis of two hind limbs); 4, paraplegia with forelimb weakness or paralysis; 5, dying or death.

Isolation lymphocytes from the central nervous system (CNS)

On day 14 after EAE induction, mice were perfused with transcardially administered PBS to eliminate contaminating blood cells in the central nervous system (CNS). The forebrain and cerebellum were dissected to expose the spinal cord, which was then carefully removed from the spinal canal. The fresh spinal cord was harvested and cut into 2 mm pieces. The CNS tissue pieces were homogenized using a syringe and passed through a 70 μM cell strainer to obtain a single-cell suspension. The single-cell suspension was digested with collagenase D (2μg/ml;11088858001; Roche) and deoxyribonuclease I (DNase I; 1 μg/ml; DN25; Sigma-Aldrich) at 37°C for 20 minutes under rotation. After digestion, the cell suspension was centrifuged to pellet the cells. The cell pellets were resuspended in 40% Percoll and layered onto a discontinuous Percoll gradient. Centrifugation at 80% Percoll allowed for the separation of cells at the 40–80% Percoll interface, which were collected as CNS mononuclear cells. The collected CNS mononuclear cells were washed with PBS to remove any remaining Percoll. CNS mononuclear cells were stimulated for 4 hours with PMA and ionomycin in the presence of Brefeldin A to induce cytokine production. After stimulation, cells were fixed, rendered permeable, and stained with appropriate antibodies for intracellular cytokine detection.

Histological analyses

The lungs, skin, liver, and colon were excised from three-week-old mice. Prior to histological analysis, the samples were fixed in formalin, embedded in paraffin, and stained with hematoxylin and eosin. For CNS histology, spinal cords were fixed in 4% paraformaldehyde, paraffin-embedded, sectioned, and stained with Luxol Fast Blue and hematoxylin and eosin (H&E). To examine colon histology, colons from *Rag1*$^{-/-}$ hosts were similarly processed and stained with H&E.

Adoptive transfer colitis model

Colitis was induced following the protocol described[25]. In brief, $CD4^+$ YFP^+ T_{reg} cells were isolated from 3-week-old $CD45.2^+$*Foxp3*^{cre}*Cxxc1*$^{fl/fl}$ and $CD45.2^+$ *Foxp3*^{cre} mice. A total of 2×10^5 T_{reg} cells from each group were mixed with 4×10^5 T_{eff} cells ($CD45.1^+CD4^+CD45RB^{hi}$) sorted from $CD45.1^+$ mice and transferred into the *Rag1*$^{-/-}$ mice via intraperitoneal injection. T_{eff} cells alone were transferred as a control group. Mouse body weight was measured weekly post-adoptive transfer. The percentage change in body weight was calculated by comparing the current weight with the initial weight on day 0. Mice were euthanized when any had reached 80% of their initial body weight. The large intestines were sectioned into 4μm thick slices and stained with hematoxylin.

In vitro T_{reg} suppression assay

Naïve $CD4^+$ T cells isolated from WT mice were labeled with CFSE (C34554; Invitrogen). $CD4^+YFP^+$ T_{reg} cells from *Foxp3*^{cre} and *Foxp3*^{cre}*Cxxc1*$^{fl/fl}$ mice were cultured with naïve $CD4^+$ T cells (1×10^5 cells) at various ratios in the presence of 2μg/mL anti-CD3(16-0031-85; Invitrogen) and 3μg/mL anti-CD28(16-0281-85; Invitrogen). On day 3, cells were analyzed by flow cytometry.

CUT&Tag

CUT&Tag assays of $CD4^+YFP^+$ T_{reg} cells were conducted as previously described[26]. Briefly, approximately 1×10^5 single cells were carefully pipetted into wash buffer twice. The pelleted cells were resuspended in wash buffer, activated concanavalin (BP531; Bangs Laboratories), and incubated for 15 minutes at room temperature. Cells bound to the beads were resuspended in Dig-Wash Buffer and incubated with a 1:50 dilution of primary antibodies (rabbit anti-H3K4me3, Active Motif,39016; rabbit anti-CXXC1, abcam, ab198977; rabbit anti-FOXP3, abcam, ab 150743;normal IgG, Cell Signaling, 2729) at 4 C overnight. The beads were incubated with a secondary antibody (goat anti-rabbit IgG; SAB3700883; Sigma-Aldrish) diluted 1:100 in Dig-Wash buffer for 60 minutes at room temperature. Cells were treated with Hyperactive pG-Tn5 Transposase (S602; Vazyme) diluted in Dig-300 Buffer for 1 hour at room temperature. The cells were subsequently resuspended in Tagmentation buffer (10mM MgCl2 in Dig-300 Buffer) and incubated at 37C for 1 hour. To halt tagmentation, 10μl was spiked with 0.5M EDTA, 3μl with 10%SDS, and 3μl with 20mg/ml Proteinase K and incubated at 55C for 1h. DNA library amplification was performed according to the manufacturer's instructions and purified using VAHTS DNA Clean Beads (N411; Vazyme). Libraries were sequenced on the Illumina NovaSeq platform (Annoroad Gene Technology).

CUT&Tag and ChIP-seq data analysis

FOXP3 ChIP-seq data was obtained from GSE121279. H3K27me3 ChIP-seq data was obtained from GSE14254. CUT&Tag and ChIP-seq reads were trimmed to 50 bp and aligned against the mouse genome build mm9 using Bowtie2(v2.3.4.1) with default parameters. All PCR duplicates and unmapped reads were removed. Peak calling was performed using MACS2(v2.1.1.20160309) and signal tracks for each sample were generated using the 'wigToBigWig' utility of UCSC. We classified the H3k4me3 peaks around TSSs into three groups: broad (>5 kb), medium (1-5kb), and narrow (<1 kb). The top 5% of the widest peaks were considered as broad peaks. The average intensity profiles were generated using deepTools (v2.5.4). Motif analysis was performed using the 'findmotifsGenome.pl' command inHomer2 package. Epigenetic factors were identified using the Epigenetic Factor Database(*https://epifactors.autosome.org/*) and then screened for those that exclusively regulate the expression of their target genes by modulating the deposition of H3K4me3. Genomic distribution was analyzed using the "genomation" R package. GO pathway analysis was performed using the "clusterProfiler" R package. The sequencing information of CUT&Tag data used in this study is summarized in Supplementary Table S1.

Clustering analysis

Promoters were defined as ±2 kb regions flanking the annotated TSS. Reads in promoters were counted using the “coverage” command in bedtools (v2.26.0) and further normalized to RPKM. The k-means clustering of H3K4me3 and H3K27me3 enrichment at promoters was conducted using the “kmeans” function in R.

RNA-seq and data analysis

Total RNA was extracted from sorted CD4CYFPC T_{reg} cells using the RNeasy Plus Mini Kit (Qiagen, #74134), following the manufacturer’s protocol. RNA-Seq libraries were constructed and sequenced by Haplox (Nanchang, China), using an Illumina platform with paired-end reads of 150 bp. RNA-seq data was obtained from GSE82076. Raw reads were trimmed to 50 bp and mapped to the mouse genome (mm9) using TopHat (v2.1.1) with default parameters. Only uniquely mapped reads were kept for downstream analysis. The RNA abundance of each gene was quantified using Cufflinks (v2.2.1).

Single-Cell RNA-Sequencing

A total of 300,000 sort-purified $CD4^{+}YFP^{+}$ T_{reg} cells from *Foxp3*^{cre} and *Foxp3*^{cre} *Cxxc1*$^{fl/fl}$ were resuspended in BD Pharmingen Stain Buffer (FBS) (554656; BD). Single cells were isolated using a chromium controller (BD platform, BD Bioscience) according to the manufacturer’s instructions, as previously described[27]. The single cells were labeled with sample tags using the BD Mouse Immune Single-Cell Multiplexing Kit (633793; BD). Following standard protocols, cDNA amplification and library construction were performed to generate scRNA-seq libraries.

Targeted scRNA-seq data processing

The raw FASTQ files were processed by BD Rhapsody using the Targeted analysis pipeline. After alignment and filtering, the distribution-based error correction(DBEC)-adjusted molecules were loaded into R studio(version 4.3.2). All subsequent analyses were performed using the package Seurat (version 4.4.0) with default parameters. Specifically, the scRNA-seq data counts were log-normalized. All targeted genes were scaled and then were used for Principal components analysis (PCA). The batch effects were removed by the HarmonyMatrix function in the Harmony package (version 1.1.0). The first 20 principal components were used to calculate nonlinear dimensionality reduction using RunUMAP. Differential gene expression (DEGs) between clusters was assessed using the FindAllMarkers function. The clusters were then annotated based on DEGs. Barplots were generated using ggplot2 (version 3.4.4). Heatmaps were generated using pheatmap (version 1.0.12).

Analysis of the single-cell TCR-seq repertoire

Raw V(D)J fastq reads were processed using BD Rhapsody Pipeline and then were analyzed using scRepertoire (version 1.12.0). The TCR clonotype was called using the nucleotide sequence of the CDR3 region for both TCR alpha and beta chains. For cells with multiple chains, the top two clonotypes with the highest expression were selected for downstream analysis. Clonal overlap between different cell types was calculated using the clonalOverlap function of scRepertoire. A clonotype was defined as expansion if it could be detected in at least two cells.

scRNA-seq trajectory analysis

UMAP embeddings obtained from the Seurat package were projected into the Slingshot(version 2.10.0) package to construct pseudotime Trajectories for T_{reg} cells. Naïve subsets were set as the root state.

Whole genome bisulfite sequencing (WGBS) and data analysis

Sorted $CD4^+YFP^+$ T_{reg} cells (3×10^6) were lysed in cell lysis buffer to release DNA. The bisulfite-treated DNA was used to prepare the sequencing library. DNA libraries were transferred to the Illumina Platform for sequencing using 150 bp paired-end reads. Raw reads were trimmed using TrimGalore (v0.4.4) with default parameters. Subsequently, the reads were mapped against the mm9 reference genome using Bismark v0.19.0 with parameters '--bowtie2'. PCR duplicates were removed and the methylation levels were calculated using 'bismark_methylation_extractor'. We calculated the mean CpG methylation levels of various genome elements: promoter, 5'-UTR, exon, intron, 3'-UTR, genebody, intergenic, CGIs, and repeats using in-house scripts. The sequencing information of WGBS data used in this study is summarized in Supplementary Table S2.

Statistical analysis

The statistical significance analysis was performed using Prism 8.0 (GraphPad). Error bars are presented as mean ± SD. *P* values of < 0.05 were deemed statistically significant (*P < 0.05, **P < 0.01, ***P < 0.001 and ****P < 0.000). Statistical analyses were performed with unpaired Student's *t*-test or two-way ANOVA and Holm–Sidak post hoc test.

Results

FOXP3 binds regulatory loci primed for activation and repression in T_{reg} cells

FOXP3-mediated gene expression is well-recognized, with several studies highlighting its dual role as both a transcriptional activator and repressor [28–32]. However, the mechanisms by which FOXP3 regulates T_{reg}-specific gene transcription via epigenetic modifications remain incompletely understood. To investigate these mechanisms, we employed CUT&Tag to generate genome-wide H3K4me3 maps in T_{reg} cells. To complement this, we compared our data with an H3K27me3 ChIP-Seq dataset from Wei *et al.*[33] focusing on previously identified FOXP3-bound loci(Konopacki *et al.* 2019)[34]. This integrative analysis allowed us to identify FOXP3-dependent genes associated with either H3K4me3 (indicative of transcriptional activation) or H3K27me3 (indicative of repression) deposition. These findings provide insight into how FOXP3 modulates the epigenetic landscape to regulate T_{reg} cell function. As expected, H3K4me3 was enriched at gene promoters (**fig. S1, A** and **B**). A Venn diagram revealed overlap between FOXP3 binding sites and H3K4me3 peaks, with minimal overlap with H3K27me3 peaks (**Fig. 1, A** and **B**). The overlapping regions between FOXP3 binding sites and H3K4me3 or H3K27me3 peaks were predominantly located at promoters (**Fig. 1, A** and **B**). To further investigate the role of FOXP3 in promoting H3K4me3 deposition, we compared H3K4me3 levels between FOXP3-positive T_{reg} cells and FOXP3-negative conventional T cells (Tconv). Consistent with our hypothesis, H3K4me3 abundance was higher at T_{reg}-specific gene loci (e.g., *Tnfrsf18*, *Ctla4*, *Il2ra* and *Nt5e*) in T_{reg} cells compared to Tconv cells (**Fig. 1,C** and **fig. S1, C**). Notably, the selection of these loci was guided by prior studies identifying genes specifically associated with T_{reg} cell function[35]. This finding highlights the role of FOXP3 in shaping the epigenetic landscape of T_{reg} cells through enhanced H3K4me3 deposition at these critical loci.

To further characterize these modifications,we clustered promoters into four groups based on the enrichment of H3K4me3 and H3K27me3. Clusters 1 and 3 showed strong enrichment of H3K4me3; cluster 2 was enriched with H3K27me3; and cluster 4 showed weak enrichment of both modifications. FOXP3 preferentially bound to clusters 1 and 3 prom-oters, which displayed high H3K4me3 levels (**Fig. 1C**). Correspondingly, genes in these clusters exhibited high transcription

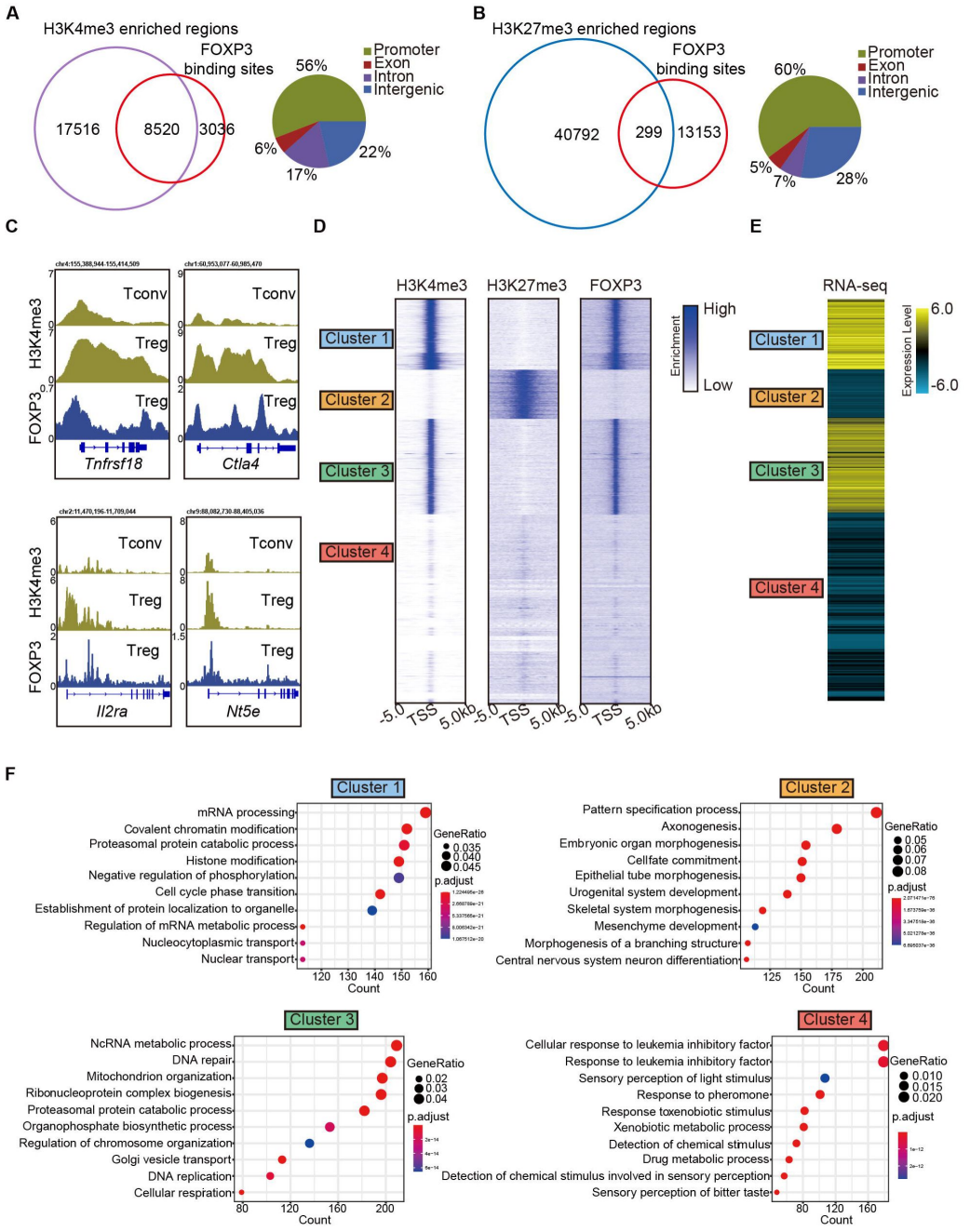

Fig. 1.

H3K4me3 is required for FOXP3-dependent gene activation in T_{reg} cells.

(**A**) Venn diagram showing overlap of H3K4me3 enriched regions (this study) and FOXP3 binding sites (Konopacki *et al.*2019) in sorted $CD4^{+}YFP^{+}T_{reg}$ cells (left). Genomic distribution of overlapped peaks(right). Note that the overlapped peaks are predominantly enriched at promoters.
(**B**) Venn diagram showing overlap of H3K27me3 enriched regions (Wei *et al.*2009) and FOXP3 binding sites in T_{reg} cells (left). Genomic distribution of overlapped peaks (right). Note that the overlapped peaks are predominantly enriched at promoters.
(**C**) Representative genome browser view showing the enrichments of H3K4me3 and FOXP3 inTconv or T_{reg} cells.
(**D**) Heatmap showing enrichment of H3K27me3, H3K4me3, and FOXP3 surrounding the TSS. Unsupervised K-means clustering was conducted on H3K27me3 and H3K4me3 signals. (**E**)Heatmap showing gene expression levels in T_{reg} cells (RNA-seq data was obtained from Oh *et al.*2017) The clusters were consistent as in **Fig. 1C**.
(**E**) Gene Ontology (GO) pathway analysis of different clusters.

levels, as shown by reanalysis of previously published RNA-seq data (Oh *et al.* 2017) [36] (**Figure 1D**, right). In contrast, genes with H3K27me3 enrichment at their promoters were transcribed at low levels.

Gene Ontology (GO) analysis of these four clusters revealed distinct functional roles. Cluster 1 was enriched in genes involved in mRNA processing, covalent chromatin modification, and histone modification, while cluster 3 was enriched in genes related to DNA repair and mitochondrion organization (**Fig. 1E**). Cluster 2, enriched with H3K27me3, was associated with pattern specification process, while cluster 4 showed no correlation with T_{reg} cells. Notably, signature T_{reg} cell genes such as *Tnfrsf18*, *Nrp1*, *Stat5a*, *Lag3*, *Icos*, and *Pdcd1* were enriched in clusters 1 and 3, showing strong H3K4me3 marks (**fig. S1C**). Conversely, genes like *Hic1*, *Trp73,* and *Rnf157*, associated with inflammatory responses, were enriched for H3K27me3 in clusters 2 (**fig. S1C**). These findings collectively support the conclusion that FOXP3 contributes to transcriptional activation in T_{reg} cells by promoting H3K4me3 deposition at target loci, while also regulating gene expression directly or indirectly through other epigenetic modifications.

CXXC1 interacts with FOXP3 and binds H3K4me3-enriched sites in T_{reg} cells

We conducted an enrichment analysis of known motifs at the overlapping peaks of FOXP3 ChIP-seq and H3K4me3 CUT&Tag in T_{reg} cells to identify epigenetic factors that directly interact with FOXP3 to mediate chromatin remodeling and transcriptional reprogramming. Motif analysis of the overlapping peaks between FOXP3 binding sites and regions enriched in H3K4me3 revealed that, in addition to transcription factors, the most abundant motif associated with H3K4me3 was the epigenetic factor CXXC1(**fig. S2A**). To investigate this further, we performed CUT&Tag for endogenous CXXC1 in T_{reg} cells to examine the genome-wide co-occupancy of CXXC1 and FOXP3. Over half of these CXXC1 binding sites were located at promoter regions (**fig. S2B**). Additionally, CXXC1 exhibited strong binding at transcription start site (TSS) and CpG islands (CGIs)(**Fig. 2A** and **fig. S2C**). As illustrated by the Venn diagram (**Fig. 2B**), more than half of the FOXP3-bound genes and H3K4me3-enriched genes were also bound by CXXC1. Similarly, more than half of CXXC1 peaks were overlapped with FOXP3 peaks (**fig. S2D**). Furthermore, the CXXC1-specific and FOXP3-specific binding sites also demonstrated modest binding of FOXP3 and CXXC1, respectively (**Fig. 2C**). These findings indicate that FOXP3 and CXXC1 share a substantial number of target genes in T_{reg} cells. To confirm this interaction, we further validated the reciprocal immunoprecipitation of both endogenous and exogenous CXXC1 and FOXP3 (**Fig. 2D and fig**. **S2E**). An immunofluorescence assay revealed predominant colocalization of CXXC1 with FOXP3 in the nucleus (**Fig. 2E**). Overall, these results suggest that CXXC1 primarily functions as a coactivator of FOXP3-driven transcription in T_{reg} cells.

Complete ablation of *Cxxc1* in T_{reg} cells leads to a fatal autoimmune disease

To investigate the role of CXXC1 in T_{reg}-cell homeostasis and function, we generated $Foxp3^{Cre}Cxxc1^{fl/fl}$ mice (conditional knockout [cKO] mice) by crossing $Cxxc1^{fl/fl}$ with $Foxp3^{YFP\text{-}Cre}$ [37] mice, thereby specifically deleting *Cxxc1* in T_{reg} cells. The effective depletion of *Cxxc1* in T_{reg} cells was confirmed through quantitative PCR (qPCR) and Western blotting (**fig. S3A**). Notably, cKO mice appeared normal at birth but later exhibited spontaneous mortality starting around three weeks of age (**Fig. 3A**). Deletion of *Cxxc1* in T_{reg} cells led to the development of severe inflammatory disease, characterized by reduced body size, stooped posture, crusting of the eyelids, ears, and tail, and skin ulceration, particularly on the head and upper back (**Fig. 3, B** and **C**). Additionally, cKO mice developed extensive splenomegaly and lymphadenopathy (**Fig. 3D**). $Foxp3^{Cre}Cxxc1^{fl/fl}$ mice exhibited elevated serum levels of anti-dsDNA autoantibodies and IgG , along with a modest increase in IgE concentration (**Figure 3E** and **fig. S3B**). Histopathological

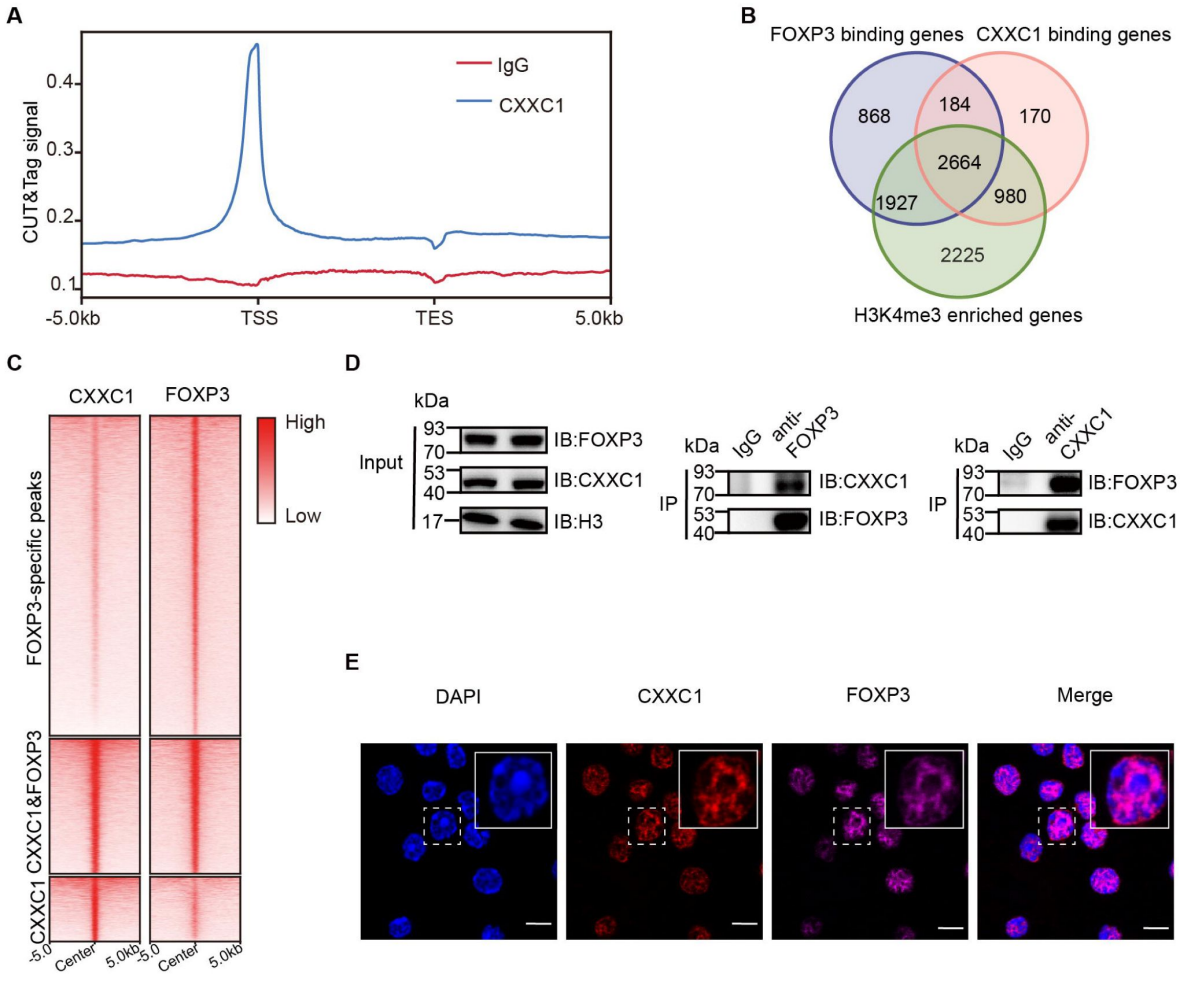

Fig. 2.

CXXC1 interacts with FOXP3 in T_{reg} cell.

(**A**) Average CXXC1 CUT&Tag signals around promoters in T_{reg}cells. IgG was used as the control.
(**B**) Venn diagrams showing the overlap of FOXP3 binding genes, CXXC1 binding genes, and H3K4me3 enriched genes in T_{reg} cells. Gene promoters covered by FOXP3 binding sites, CXXC1 binding sites, or exhibited high H3K4me3 levels were defined as FOXP3-bound genes, CXXC1-bound genes, or H3K4me3-enriched genes.
(**C**) Heatmaps showing FOXP3 ChIP-seq and CXXC1 CUT&Tag signals at indicated regions.
(**D**) Interaction between FOXP3 and CXXC1 was assessed by co-IP (forward and reverse) using T_{reg} cell lysates.
(**E**) Immunofluorescence for FOXP3 and CXXC1 colocalization in T_{reg} cells. Scale bars, 2 μm.

analysis revealed massive lymphocyte and myeloid cell infiltration in the skin, lungs, liver sinusoids, and colon mucosa (**Fig. 3F**). In full agreement with the aforementioned severe autoimmune diseases, *Foxp3*^{Cre}*Cxxc1*$^{fl/fl}$ mice had decreased percentages and numbers of CD4^{+} Foxp3^{+} T_{reg} cells in small intestine lamina propria (LPL), liver and lung(**Fig. 3G and fig**. **S3C**). Moreover, cKO mice displayed an increase in CD8^{+} T cell percentages (**fig. S3D**), along with a marked rise in cells exhibiting an effector/memory phenotype (CD44hi CD62Llo) (**Fig. 3H**). Furthermore, T cells from cKO mice produced elevated levels of IFN-γ, IL-17, and IL-4 in CD4^{+} YFP^{-} T cells, as well as increased IFN-γ production in CD8^{+} T cells (**Fig. 3I and fig**. **S3, E** and **F**). These phenotypes closely resembled those observed in *Foxp3*-deficient mice [38] or mice with depleted T_{reg} cells[39], suggesting a deficiency in immune suppression.

CXXC1 is necessary for the maintenance of T_{reg}-cell suppressive activity

Despite the development of severe autoimmune disease, we observed an increase in both the absolute number and percentage of FOXP3^{+} T_{reg} cells in the lymph nodes (**fig. S4A**). The expression level of the FOXP3 protein was only slightly altered in *Cxxc1*-deficient T_{reg} cells (**fig. S4B**). In an *in vitro* suppression assay, T_{reg} cells from *Foxp3*^{Cre}*Cxxc1*$^{fl/fl}$ and WT mice exhibited similar suppressive effects on naïve T (Tn) cell proliferation (**fig. S4C**). The expression of the hallmark T_{reg}-cell marker CTLA-4 showed a modest increase in *Cxxc1*-deficient T_{reg} cells compared to WT T_{reg} cells, while the expression of GITR remained unchanged (**fig. S4D**). To further assess the suppressive capacity of *Cxxc1*-deficient T_{reg} cells *in vivo*, we employed the experimental autoimmune encephalomyelitis (EAE) model. Naïve CD4^{+} T cells from 2D2 mice were co-transferred with T_{reg} cells from either *Foxp3*^{Cre} or *Foxp3*^{Cre} *Cxxc1*$^{fl/fl}$ mice into *Rag1*$^{-/-}$ recipients, and EAE was induced in these recipient mice. Mice that received only naïve CD4^{+} T cells from 2D2 mice developed more severe EAE symptoms (**Fig. 4A**). The addition of WT T_{reg} cells from *Foxp3*^{Cre} mice slightly mitigated EAE progression and reduced Th17 cells in the spinal cord (**Fig. 4, A** to **D**). In contrast, *Foxp3*^{Cre} *Cxxc1*$^{fl/fl}$ T_{reg} cells failed to suppress EAE (**Fig. 4, A** to **D**), and the cKO mice showed a reduction in T_{reg} cells frequency in CNS tissues(**Fig. 4E**). Finally, we examined the role of CXXC1 in T_{reg} cell-mediated suppression using T cell transfer-induced colitis, in which naïve T cells were transferred to *Rag1*$^{-/-}$ recipients either alone or together with WT or *Foxp3*^{Cre} *Cxxc1*$^{fl/fl}$ T_{reg} cells. The transfer of naïve T cells led to weight loss and intestinal pathology in recipient mice(**Fig. 4, F** and **G**). Mice receiving WT T_{reg} cells continued to gain weight (**Fig. 4F**) , whereas those that received T_{reg} cells from cKO mice were unable to prevent colitis and exhibited a reduced percentage of T_{reg} cells (**Fig. 4, F** to **H**). These findings underscore the critical role of CXXC1 in maintaining T_{reg} cell function *in vivo*.

T_{reg} cell lineage homeostasis and proliferation depend upon CXXC1

T_{reg} cells harbor a diverse T-cell receptor (TCR) repertoire, which likely play a critical role in their immune suppression function [40–42]. To explore the role of CXXC1 in T_{reg}-mediated suppression, we performed single-cell RNA sequencing (scRNA-seq) combined with TCR sequencing (TCR-seq) on CD4^{+}YFP^{+} T_{reg} cells isolated from mouse lymph nodes. After quality control and removal of doublets, 18,577 cells were retained for further analysis. Through unsupervised clustering and uniform manifold approximation and projection (UMAP) analysis, we identified eight distinct T_{reg} cell clusters based on the expression of well-characterized markers, with a particular focus on two clusters of activated T_{reg} cells that exhibited higher expression of markers and gene sets relative to naïve T_{reg} cells (**Fig. 5A** and **fig. S5, A** to **C**). A comparison between *Cxxc1*-deficient and WT T_{reg} cells within each cluster revealed a reduction in *Cxxc1*-deficient cells in the naïve subsets, while an increase was observed in the Gzmb^{+} and H2-Eb1^{+} subsets (**Fig. 5B**). To further elucidate the transition of T_{reg} cells along a dynamic biological timeline, we constructed pseudo-time trajectories using Slingshot [43]. The pseudo-time gradient depicted a progression from quiescent to activated T_{reg} cells, ultimately encompassing the Gzmb^{+}

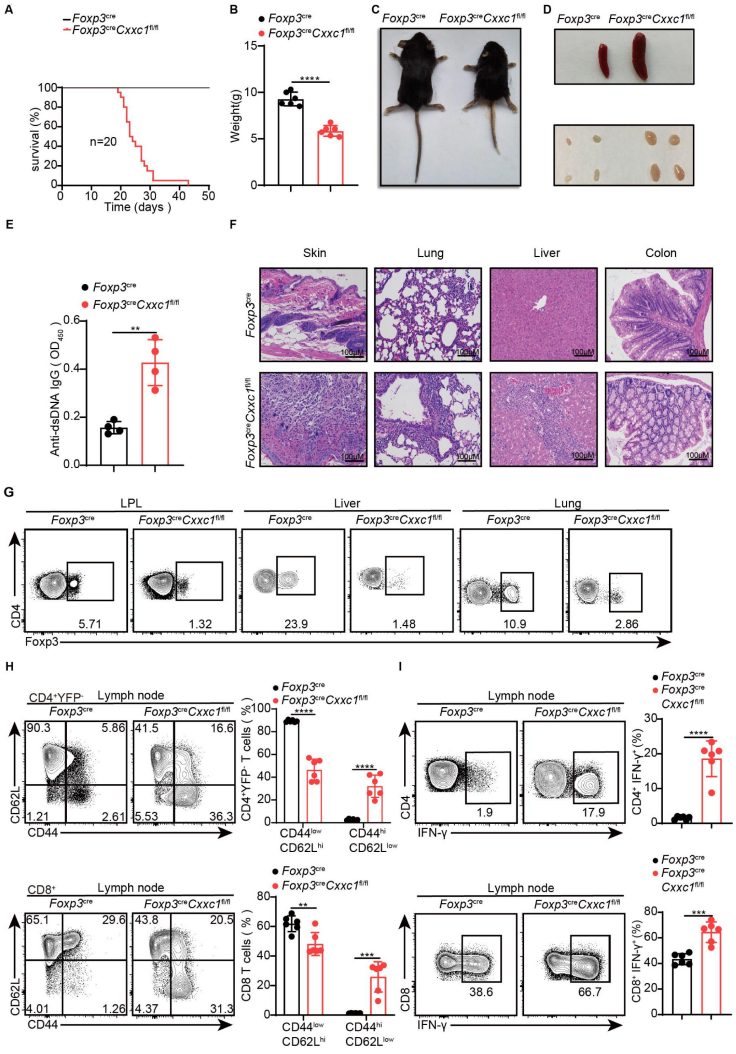

Fig. 3.

Foxp3creCxxc1$^{fl/fl}$ mice spontaneously develop a fatal early-onset inflammatory disorder.

(**A**) Survival curves of *Foxp3*^{cre} (black line) and *Foxp3*^{cre}*Cxxc1*$^{fl/fl}$ (red line) mice (*n* = 20).
(**B**) Gross body weight of *Foxp3*^{cre} and *Foxp3*^{cre}*Cxxc1*$^{fl/fl}$ mice (*n*C=C6).
(**C**) A representative image of *Foxp3*^{cre} and *Foxp3*^{cre}*Cxxc1*$^{fl/fl}$ mice.
(**D**) Representative images showing the spleen and peripheral lymph nodes from *Foxp3*^{cre} and *Foxp3*^{cre}*Cxxc1*$^{fl/fl}$ mice.
(**E**) ELISA quantification of anti-dsDNA IgG in the serum of *Foxp3*^{cre} and *Foxp3*^{cre}*Cxxc1*$^{fl/fl}$ mice (n = 4).
(**F**) Hematoxylin and eosin staining of the skin, lung, liver, and colon from *Foxp3*^{cre} an d *Foxp3*^{cre}*Cxxc1*$^{fl/fl}$ mice (scale bar, 100Cμm).
(**G**) Representative flow cytometry plots of CD4C Foxp3C T_{reg} cells isolated from the small intestinal lamina propria (LPL), liver, and lung of *Foxp3*^{cre} and *Foxp3*^{cre}*Cxxc1*$^{fl/fl}$ mice.
(**H**) Flow cytometry analysis of CD62L and CD44 expression on peripheral lymph node CD4^{+}YFP^{-} and CD8^{+}T cells from *Foxp3*^{cre} and *Foxp3*^{cre}*Cxxc1*$^{fl/fl}$ mice (left). Right, frequency of CD44^{low}CD62L^{hi} and CD44^{hi}CD62L^{low} population in CD4^{+} YFP^{-} or CD8^{+} T cells (*n* = 6).
(**I**) Lymph node cells from *Foxp3*^{cre} and *Foxp3*^{cre}*Cxxc1*$^{fl/fl}$ mice were stimulated ex vivo with PMA + ionomycin for 4h and analyzed for IFN-γ expressing in CD4^{+} YFP^{-} or CD8^{+} T cells using flow cytometry (left). Right, percentages of IFN-γ^{+}CD4^{+} YFP^{-} or IFN-γ^{+}CD8^{+} T cells in the lymph nodes of *Foxp3*^{cre} and *Foxp3*^{cre}*Cxxc1*$^{fl/fl}$ mice (*n* = 6).
All mice analyzed were 18-20 days old unless otherwise specified. Error bars show mean ± SD. The log-rank survival curve was used for survival analysis in A, and multiple unpaired *t*-test or two-tailed Student's *t*-test were used for statistical analyses in B, E, Gand H (***P*<0.01, ****P*C<C0.001, *****P*<0.0001). The flow cytometry results are representative of three independent experiments.

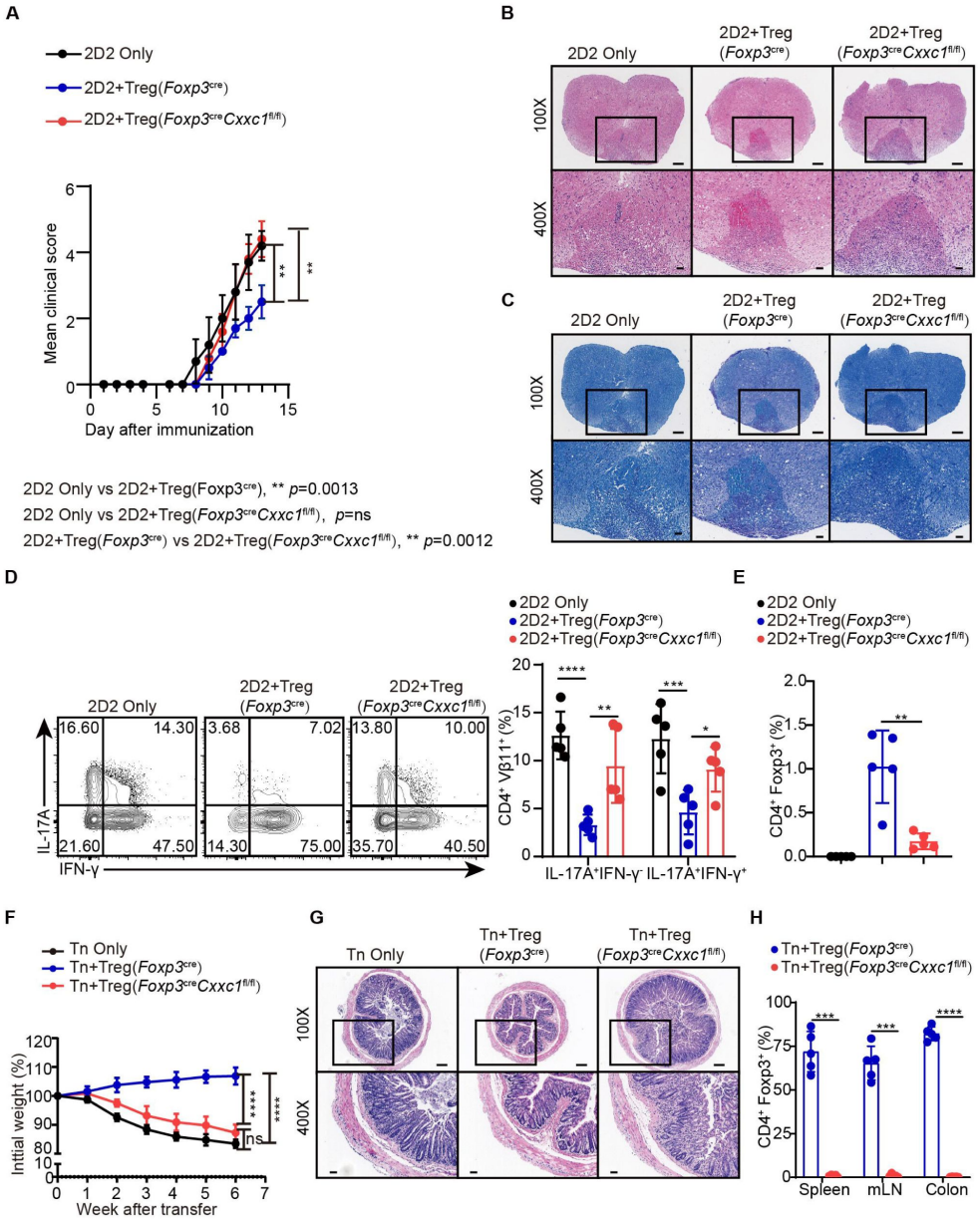

Fig. 4.

CXXC1 is essential for T_{reg} cells to suppress T cell-mediated EAE and colitis.

(**A**)Mean clinical scores for EAE in *Rag1*$^{-/-}$ recipients of 2D2 CD4$^+$ T cells, either alone or in combination with *Foxp3*^{cre} or *Foxp3*^{cre}*Cxxc1*$^{fl/fl}$ mice after immunization with MOG35–55, complete Freund's adjuvant (CFA), and pertussis toxin (n=5). (**B** and **C**)Representative histology of the spinal cord of *Rag1*$^{-/-}$ mice after EAE induction. Hematoxylin and eosin(H&E) staining (upper), Luxol fast blue (F&B) staining (lower). Scale bars, 50 μm (400×) and 200 μm (100×).
(**D**) Representative flow cytometry plots and quantification of the the percentages of IFNγ$^+$ or IL-17A$^+$ CD4$^+$Vβ11$^+$ T cells (n=5).
(**E**) Statistical analysis of the percentage CD4$^+$ FOXP3$^+$ T_{reg} cell in CNS tissues 14 days after EAE induction.
(**F**) Changes in body weight of *Rag1*$^{-/-}$ mice after colitis induction(n=6).
(**G**) Haematoxylin and eosin (H&E) staining of colons from T cell-induced colitis mice 6 weeks after T cell transfer. Scale bars, 50 μm (400×) and 200 μm (100×).
(**H**) Statistical analysis of the percentage CD4$^+$ FOXP3$^+$ T_{reg} cell in the spleen, mesenteric lymph nodes, and colon 6 weeks after colitis induction.
Error bars show mean ± SD. *P* values are determined by a two-tailed Student's *t*-test or two-way ANOVA and Holm–Sidak post hoc test (A, D, E and H). (*P<0.05, **P<0.01, ***PC<C0.001, ****P<0.0001).

and H2-Eb1$^+$ subsets (**Fig. 5B**). To further elucidate the transition of T_{reg} cells along a dynamic biological timeline, we constructed pseudo-time trajectories using Slingshot [43]. The pseudo-time gradient depicted a progression from quiescent to activated T_{reg} cells, ultimately encompassing the Gzmb$^+$ and H2-Eb1$^+$ subsets (**Fig. 5C**). Given the antigen-specific suppression capabilities of T_{reg} cells [44,45], we examined their clonal expansion. The analysis revealed that expanded WT TCR clonotypes (nC≥C2) were predominantly distributed among the Nt5e$^+$ subsets, while *Cxxc1*-deficient T_{reg} cells showed expanded clonotypes primarily within the Gzmb$^+$ and H2-Eb1$^+$ subsets(**Fig. 5D** and Fig. S5D). TCR sharing analysis indicated clonotype sharing among various clusters of WT T_{reg} cells, suggesting a degree of homogeneity. However, the reduced TCR sharing in *Cxxc1*-deficient T_{reg} cells implies that decreased TCR diversity may impair the suppressive activity of T_{reg} cells (**Fig. 5E**) [42]. Furthermore, the *Cxxc1*-deficient group exhibited lower expression of several T_{reg}-specific genes associated with suppressive functions, such as*Nt5e*, *Il10*, *Pdcd1*, *Klrg1*, as well as genes that inhibit effector T cells differentiation, including *Sell* and *Tcf7* (**Fig. 5F** and **fig. S5E**). Conversely, *Cxxc1*-deficient T_{reg} cells demonstrated elevated expression of *Gzmb*, *Il2ra*, and *Cd69* compared to WT, reflecting a profile indicative of increased activation (**Fig. 5, F** and **G**). Additionally, we observed increased expression of genes linked to Th1-type inflammation, such as *Ifng*, *Tbx21*, and *Hif1a*, in *Cxxc1*-deficient T_{reg} cells, likely due to extreme inflammatory conditions (**Fig. 5, F** to **H**). The proportion of FOXP3$^+$Ki67$^+$ T_{reg} cells was lower in cKO mice compared to WT mice (**Fig. 5I**). These findings underscore the crucial role of CXXC1 in in maintaining T_{reg} cell function and homeostasis.

Intrinsic *Cxxc1* deficiency impairs T_{reg} cell suppression, proliferation, and molecular programs

To confirm that the deficiency in T_{reg} cell function in T_{reg}-specific *Cxxc1*-deficient animals is due to intrinsic defects caused by *Cxxc1* deficiency, rather than severe autoimmune inflammation in *Foxp3*^{Cre} *Cxxc1*$^{fl/fl}$ mice, we examined *Cxxc1*-sufficient and *Cxxc1*-deficient T_{reg} cell subsets in heterozygous *Foxp3*$^{Cre/+}$ *Cxxc1*$^{fl/fl}$ (designated as “het-KO”) and littermate *Foxp3*$^{Cre/+}$ *Cxxc1*$^{fl/+}$ (designated as “het-WT”) female mice (**Fig. 6A**). Notably, het-KO female mice did not exhibit overt signs of autoimmunity, as random X-chromosome inactivation led to the coexistence of both *Cxxc1*-cKO and *Cxxc1*-WT T_{reg} cells. However, both the frequency and absolute numbers of FOXP3$^+$YFP$^+$ T_{reg} cells within the total T_{reg} population were reduced in het-KO mice compared to their counterparts in het-WT littermates, indicating that *Cxxc1* deficiency imposes a competitive disadvantage on T_{reg} cells (**Fig. 6B**). Additionally, *Cxxc1*-deficient YFP$^+$ T_{reg} cells failed to upregulate the proliferation marker Ki-67 (**Fig. 6C**). Moreover, YFP$^+$ T_{reg} cells in het-KO female mice showed reduced expression of key genes essential for suppressive function, including ICOS, CD25,CTLA4, and GITR, compared to YFP$^-$$T_{reg}$ cells from the same mice (**Fig. 6D**). Consistently, we confirmed the impaired suppressive function of T_{reg} cells from heterozygous *Foxp3*$^{Cre/+}$ *Cxxc1*$^{fl/fl}$ mice in *vitro* and in *vivo* (**Fig. 6E** and **fig. S6A-E**). To investigate the molecular program affected by the deletion of *Cxxc1* in T_{reg} cells, we performed RNA-sequencing (RNA-seq) analysis on CD4$^+$YFP$^+$ T_{reg} cells isolated from het-WT and het-KO mice. We then conducted a differential gene expression (DGE) analysis based on the RNA-seq data. Among all expressed genes, 865 were upregulated (“Up” genes) and 761 were downregulated (“Down” genes) by ≥1.5-fold in CD4$^+$YFP$^+$ T_{reg} cells from het-KO mice compared to het-WT mice, with a false discovery rate (FDR)–adjusted *P*-value cutoff of 0.05 (**fig. S6F**). Gene Ontology (GO) enrichment analysis revealed that the downregulated genes in *Cxxc1*-deficient T_{reg} cells were predominantly enriched in pathways related to the negative regulation of immune system process and regulation of cell–cell adhesion (**fig. S6G**). The *Cxxc1*-deficient T_{reg} cells also showed reduced expression of several genes associated with T_{reg} cell suppressive function, including *Il10*, *Tigit*, *Lag3*, *Icos*, *Nt5e*(encoding CD73) and *Itgae* (encoding CD103) (**fig. S6H**). Thus, while YFPC WT T_{reg} cells effectively prevent autoimmunity in het-KO mice, the absence of *Cxxc1* in YFPC T_{reg} cells disrupts key T_{reg} cell marker expression and impairs their suppressive function under steady-state conditions.

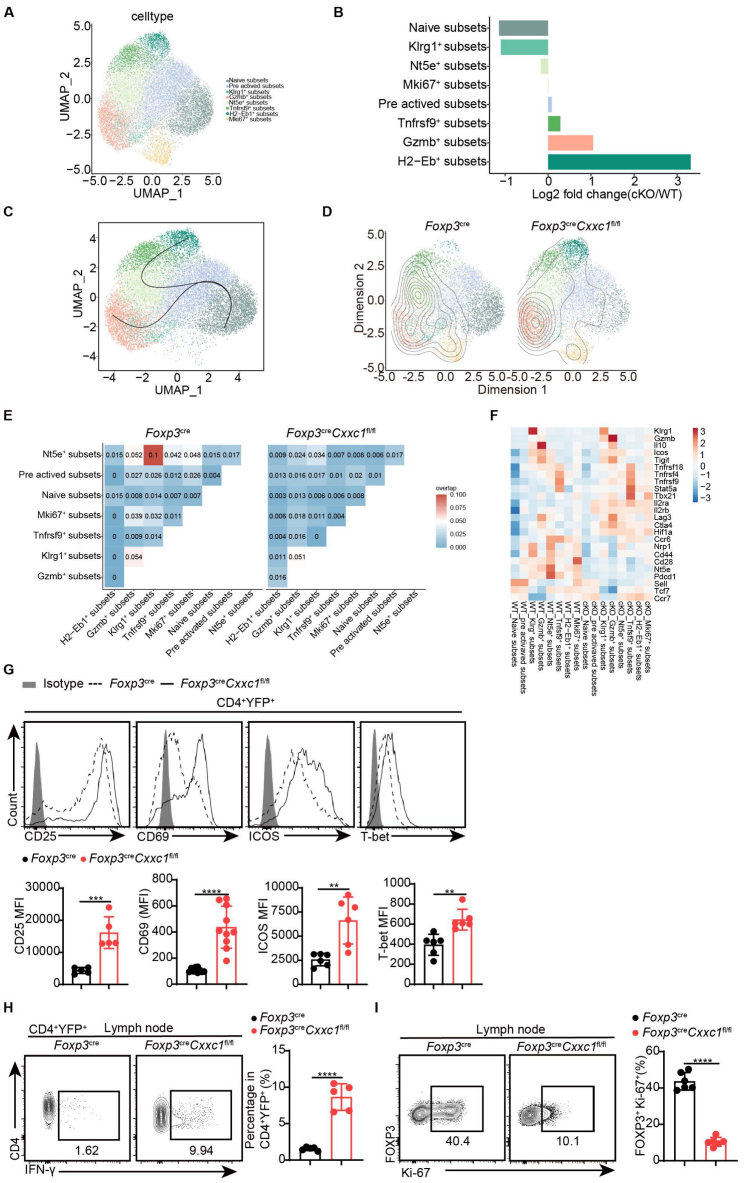

Fig. 5.

Single-cell transcriptomics reveals distinct T_{reg} cell populations.

(**A**) UMAP plot showing clusters identified based on variable gene expression of sorted $CD4^+YFP^+$ T_{reg} cells. Each dot represents a cell, and each color corresponds to a different population of cell types. Clustering analysis revealed 8 distinct T_{reg} cell populations.
(**B**) Mean fold changes in cluster abundance between *Foxp3*^{cre} and *Foxp3*^{cre}*Cxxc1*$^{fl/fl}$ mice. (**C**)Pseudotime trajectories of T_{reg} cells based on Slingshot, color-coded by T_{reg} cell subpopulations.
(**D**) Visualization of density and clonotype richness across T_{reg} clusters from *Foxp3*^{cre} and *Foxp3*^{cre}*Cxxc1*$^{fl/fl}$ mice.
(**E**) TCR sharing of expanded clonotypes across all possible combinations of T_{reg} cells from *Foxp3*^{cre} and *Foxp3*^{cre}*Cxxc1*$^{fl/fl}$ mice.
(**F**) Heatmap showing Z scores for the average expression of T_{reg}-specific genes in each cluster between *Foxp3*^{cre} and *Foxp3*^{cre}*Cxxc1*$^{fl/fl}$ mice.
(**G-H**)Representative flow cytometry plots and quantification of (G) expression of CD25, CD69, ICOS, T-bet, and (H) IFN-γ in $CD4^+YFP^+$ T_{reg} cells from *Foxp3*^{cre} and *Foxp3*^{cre}*Cxxc1*$^{fl/fl}$ mice (n=5 CD25, n=10 CD69, n=5 ICOS, n=6 T-bet, n=5 IFN-γ).
(**I**)Ki-67 expression (left) and frequency (right) in $CD4^+FOXP3^+$ T_{reg} cells from *Foxp3* ^{cre} a-nd *Foxp3*^{cre}*Cxxc1*$^{fl/fl}$ mice (n=6).
Error bars show mean ± SD. *P* values are determined by a two-tailed Student's *t*-test (G-I). (***P*<0.01, ****P*<0.001, *****P*<0.0001). The flow cytometry results are representative of three independent experiments.

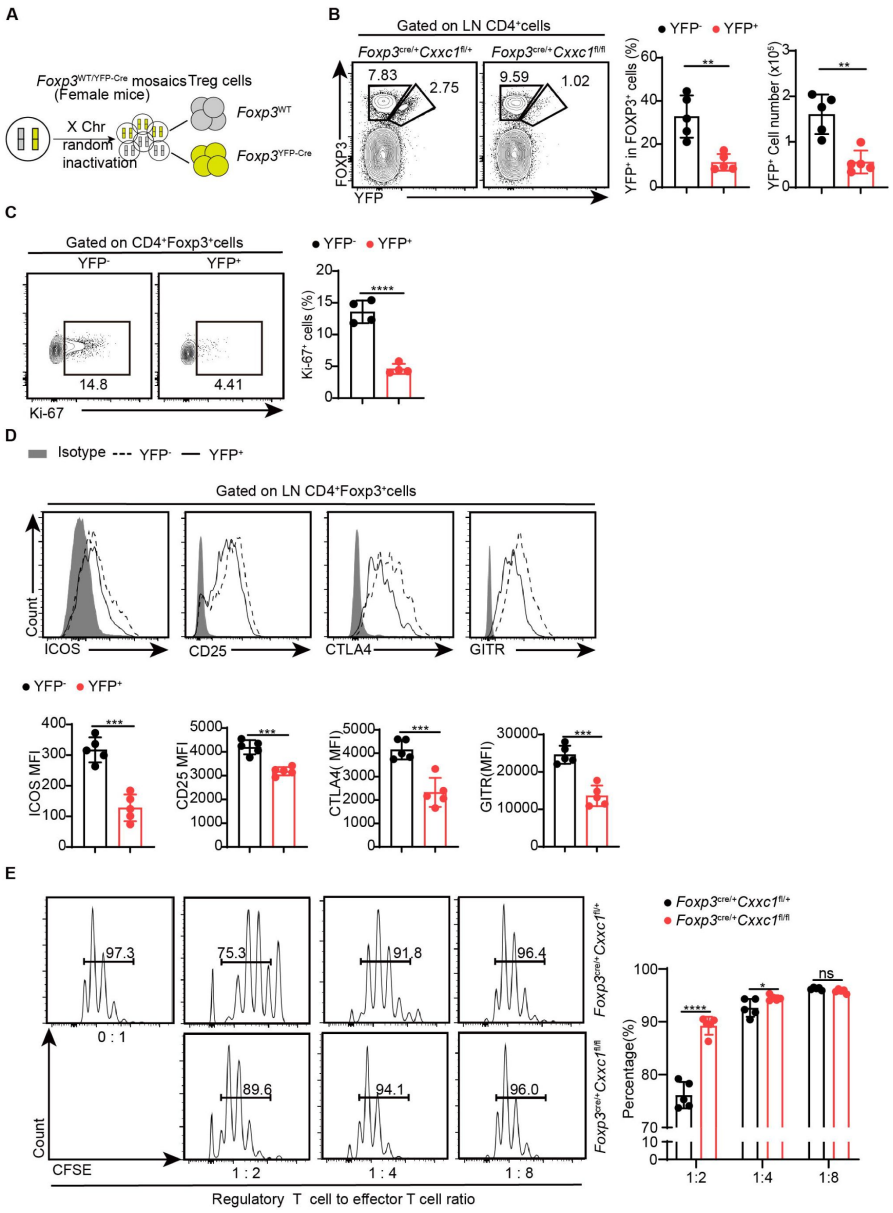

Fig. 6.

Cxxc1-deficient T_{reg} cells exhibit functional impairment and disrupted homeostasis in steady-state conditions.

(**A**) Schematic representation of wild-type and Cre-positive T_{reg} cells in female *Foxp3*$^{Cre/+}$mice.
(**B**) Flow cytometry analysis of the YFP^{-}FOXP3^{+} (WT) and YFP^{+}FOXP3^{+} (KO) T_{reg} cells in *Foxp3*$^{Cre/+}$ *Cxxc1*$^{fl/+}$ (het-WT) and *Foxp3*$^{Cre/+}$ *Cxxc1*$^{fl/fl}$ (het-KO) female mice (left), along with the frequency and absolute numbers of YFP^{+} cells within the total T_{reg} population (right)(n=5).
(**C**) Flow cytometry analysis of Ki-67expression (left) and MFI (right) in YFP^{-} and YFP^{+} cells within the CD4^{+}FOXP3^{+} T_{reg} cells from 6- to 8-week-old het-KO female mice (n=4).
(**D**)Representative flow cytometry plots and quantification of ICOS, CD25, CTLA4, and GITR expression in YFP^{-} and YFP^{+} cells within CD4^{+}FOXP3^{+} T_{reg} cells from het-KO female mice (n=5).
(**E**)Suppression of CFSE-labelled Tn cell proliferation by different ratios of CD4^{+}YFP^{+} T_{reg} cells from *Foxp3*$^{Cre/+}$ *Cxxc1*$^{fl/+}$ and *Foxp3*$^{Cre/+}$ *Cxxc1*$^{fl/fl}$ female mice. On the right, the percentage of proliferated responding T cells is presented (n=5).
Error bars show mean ± SD. *P* values are determined by a two-tailed Student's *t*-test (B-E). (ns, not significant. *P<0.05,**P<0.01, ***PC<C0.001, ****P<0.0001). The flow cytometry results are representative of three independent experiments.

The FOXP3-CXXC1 complex regulates the expression of key factors in T_{reg} cells that are associated with the breadth of H3K4me3

CXXC1 binds to unmethylated CpG DNA via its N-terminal CXXC finger domain, facilitating its interaction with DNA methyltransferase 1 (DNMT1). This binding stabilizes the DNMT1 protein, thereby regulating DNA methylation [46,47]. To investigate whether CXXC1 depletion affects DNA methylation in T_{reg} cells, we performed whole genome bisulfite sequencing (WGBS) on T_{reg} cells isolated from both WT and cKO mice. On average, *Cxxc1*-deficient T_{reg} cells exhibited no changes in DNA methylation at gene loci or across genome-wide CpG sites, irrespective of chromosomal region (**fig. S7, A** to **C**). Furthermore, *Cxxc1* knockout T_{reg} cells did not show a increase in DNA methylation at key T_{reg} signature gene loci (**fig. S7D**). Given the pivotal role of MLL4-mediated H3K4me1 in establishing the enhancer landscape and facilitating long-range chromatin interactions during T_{reg} cell development[15], we performed CUT&Tag to assess changes in H3K4me1 levels in *Cxxc1*-deficient T_{reg} cells. This analysis revealed that H3K4me1 levels were similar in both WT and *Cxxc1*-deficient T_{reg} cells (**fig. S7, E** to **G**).

While H3K4me3 modifications typically form sharp 1-to 2-kb peaks around promoters, some genes exhibit broader H3K4me3 regions, referred to as broad H3K4me3 domains (H3K4me3-BDs), which can extend to cover part or all of the gene's coding sequences (up to 20 kb) [48,49]. Broad H3K4me3 domains are preferentially associated with genes essential for the identity or function of specific cell types [48,50] and have been implicated in enhancing transcriptional elongation and increasing enhancer activity [50]. To further explore the connection between broad H3K4me3 domains and the expression of immune-regulatory genes, we analyzed genes containing broad H3K4me3 regions. We classified the H3K4me3 domains surrounding transcription start sites (TSSs) into three categories: broad (more than 5 kb), medium (between 1 and 5 kb), and narrow (less than 1 kb) (**Fig. 7A**). Notably, *Cxxc1*-deficient T_{reg} cells exhibited weaker H3K4me3 signals compared to WT cells within the broad H3K4me3 domains where CXXC1 binding is prominent (**Fig. 7, A** and **B**). Using the criteria established by Benayoun *et al.*[48], which defines the top 5% of the widest H3K4me3 domains as BDs, we observed similar enrichment results (**fig. S7, H** and **I**). We then compared three groups of genes: BD-associated genes with reduced H3K4me3 levels following *Cxxc1* deletion, genes with direct CXXC1 binding, and genes with direct FOXP3 binding. The Venn diagram revealed that the majority of genes (283 out of 294, 96%) with CXXC1 binding and reduced H3K4me3 levels overlap with FOXP3-bound genes, suggesting that CXXC1 presence enhances FOXP3 binding within the broad H3K4me3 domain (**Fig. 7C**). Furthermore, GO term analysis indicated that BD-associated genes are enriched in biological processes related to the negative regulation of immune system processes (**Fig. 7D**). Genome browser views displayed the enrichments of FOXP3, CXXC1, and H3K4me3 at key signature genes in T_{reg} cells, such as *Ctla4, Il2ra, Icos*, and *Tnfrsf18*, with lower H3K4me3 densities observed at these loci in *Cxxc1*-deficient T_{reg} cells (**Fig. 7E**). Similar patterns were observed at core genes involved in T_{reg} homeostasis and suppressive function (e.g., *Lag3*, *Nt5e*, *Ikzf4*, and *Cd28*) (**fig. S7, J**)[51,52]. These findings suggest that CXXC1 and FOXP3 collaboratively promote sustained T_{reg} cell homeostasis and function by preserving the H3K4me3 modification at key T_{reg} cell genes.

We previously demonstrated that the FOXP3-CXXC1 complex plays a key role in modulating H3K4me3 deposition at T_{reg}-specific gene loci. To further clarify whether *Cxxc1* deletion affects FOXP3 binding to its target genes, we performed CUT&Tag experiments to compare FOXP3 binding profiles between WT and *Cxxc1* KO T_{reg} cells. The results revealed that most FOXP3-bound regions in WT T_{reg} cells were similarly enriched in KO T_{reg} cells, indicating that *Cxxc1* deletion does not impair FOXP3's DNA-binding ability (**fig. S8A** and **B**). Together, these findings suggest that the regulatory role of CXXC1 in T_{reg} cells is mediated through its effect on H3K4me3 deposition rather than altering FOXP3's binding to DNA.

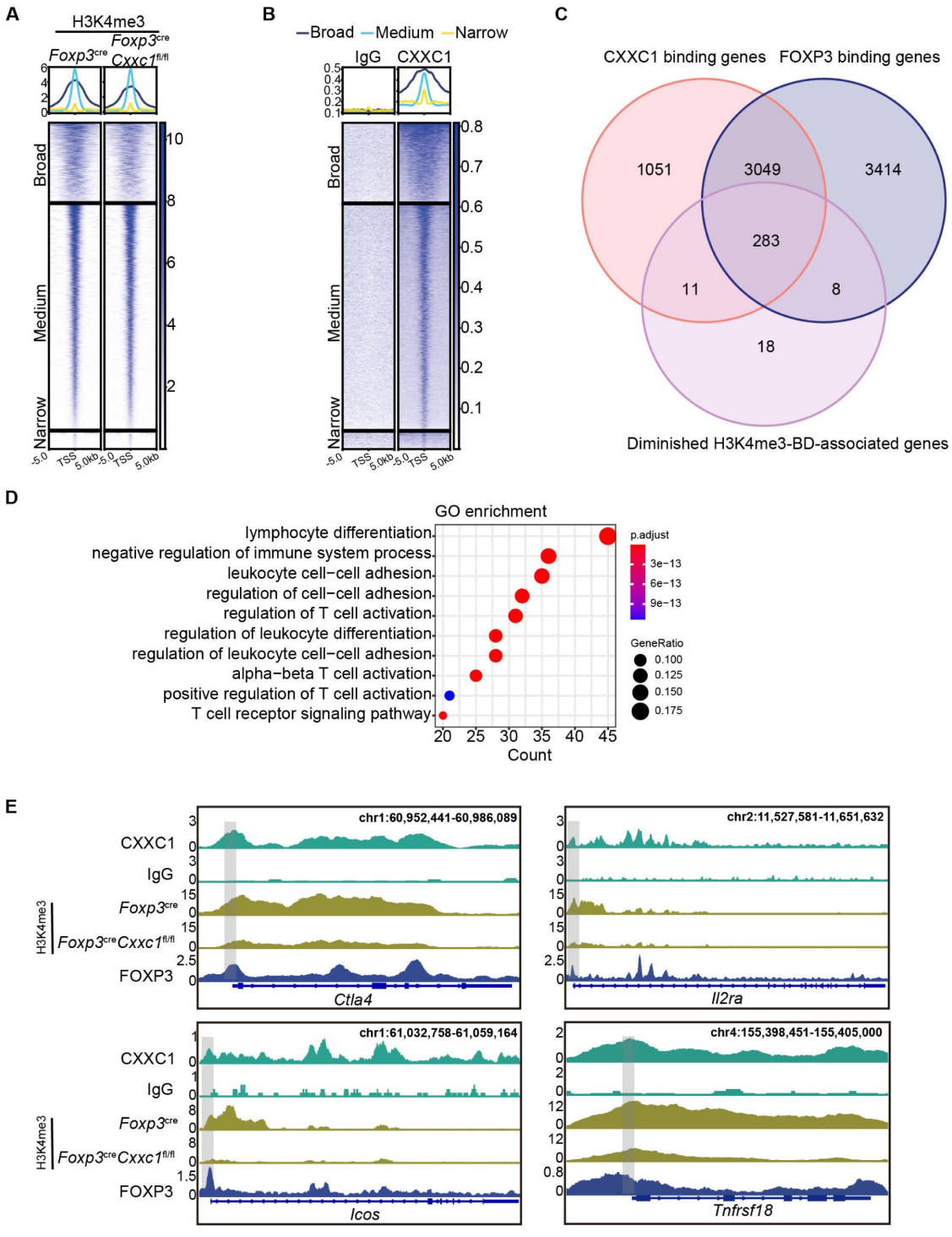

Fig. 7.

CXXC1 regulates Foxp3-dependent molecule H3K4 trimethylation in T_{reg} cells.

(**A**-**B**)Heatmaps showing H3K4me3(A)and CXXC1(B) signals centered on narrow, medium, and broad domains. The top panel shows the average CUT&Tag signals around indicated domains.
(**D**) Venn diagrams showing the overlap of FOXP3 binding genes, CXXC1 binding genes, and H3K4me3-BD-associated genes with decreased H3K4me3 levels after CXXC1 depletion in T_{reg} cells.
(**E**) Gene Ontology (GO) pathway analysis of the overlap peaks.
(**F**) Representative genome browser view showing the enrichments of FOXP3, CXXC1, and H3K4me3 in T_{reg} cells.

Discussion

T_{reg} cells specifically express the transcription factor FOXP3, which is essential for maintaining T_{reg} lineage stability and suppressive function[53]. However, FOXP3 alone is insufficient to fully regulate the transcriptional signature and functionality of T_{reg} cells; its interaction with protein partners is crucial for this regulation. In this study, we identify CXXC1 as a critical epigenetic regulator and functional cofactor of FOXP3. Although CXXC1 is not required for FOXP3's DNA-binding activity, as evidenced by similar FOXP3 binding patterns in WT and *Cxxc1*-deficient T_{reg} cells (CUT&Tag analysis), it plays an essential role in maintaining H3K4me3 modifications at FOXP3 target loci. By acting as both an epigenetic regulator and a FOXP3 cofactor, CXXC1 ensures the stability of the T_{reg} transcriptional program, highlighting its pivotal role in preserving T_{reg} cell functionality and immune homeostasis.

FOXP3 is known to promote histone H3 acetylation at the promoters and enhancers of its target genes, such as *Il2ra*, *Ctla4*, and *Tnfrsf18*, following T_{reg} cell activation, thereby functioning as a transcriptional activator[54,55]. Conversely, FOXP3 can act as a repressor by silencing target genes like *Il2* and *Ifng* through the induction of histone H3 deacetylation, mediated by the recruitment of histone deacetylases and transcriptional co-repressors[10,56]. Additionally, FOXP3 exerts this repression by recruiting the Ezh2-containing polycomb repressive complex to target genes during activation, as FOXP3-repressed genes are associated with H3K27me3 deposition and reduced chromatin accessibility[11,57]. Recent studies have begun to explore the biological significance of H3K4me3 breadth, revealing a positive correlation between H3K4me3 breadth and gene expression [50,58,59]. These studies also suggest that H3K4me3 breadth contributes to defining specific cell identities during development and disease, including systemic autoimmune diseases like systemic lupus erythematosus and various cancers [48,60–63]. Our study demonstrates that the loss of *Cxxc1* leads to reduced H3K4me3 levels, predominantly in genes with broader peaks, such as *Il2ra, Tnfrsf18, Ctla4 and Icos*, directly impairing their suppressive function in T_{reg} cells. Although our research primarily focused on the role of CXXC1 in T_{reg} cells, it is plausible that similar mechanisms may be operative in other cell types.

The T_{reg}-specific deletion of *Cxxc1* leads to a rapid and fatal autoimmune disorder, characterized by systemic inflammation and tissue damage, underscoring the essential role of CXXC1 in maintaining immune self-tolerance within T_{reg} cells. Interestingly, despite this severe phenotype, our findings show that H3K4me1 levels were comparable between WT and *Cxxc1*-deficient T_{reg} cells. In contrast, MLL4 is critical for T_{reg} cell development in the thymus, primarily by regulating H3K4me1, though it is not required for peripheral T_{reg} cell function[15]. Numerous studies investigating the effectors of T_{reg} cell-mediated suppression have identified a wide range of molecules and mechanisms. These include the upregulation of the inhibitory co-stimulatory receptor CTLA-4, which initiates inhibitory signaling; the sequestration of the T-cell growth factor IL-2 via CD25; the secretion of inhibitory cytokines, such as interleukin (IL)-10, IL-35 and TGF-β and the activity of ectoenzymes CD39 and CD73 on the T_{reg} cells surface, which convert extracellular ATP, a potent pro-inflammatory mediator, into its anti-inflammatory counterpart, adenosine[42,64]. Mechanistically, we demonstrated that CXXC1 interacts with FOXP3 to regulate T_{reg} cell function by trimethylating H3K4 at broad H3K4me3 domains of multiple genes involved in suppressive functions such as *Il2ra, Nt5e, and Ctla4*. Additionally, MLL1, another KMT, controls T_{reg} cell activation and function by specifically regulating H3K4 trimethylation at genes encoding key T_{reg}-related molecules such as *Tigit*, *Klrg1*, *Tbx21*, *Cxcr3*, and serves as a crucial epigenetic regulator in establishing a stable Th1-T_{reg} lineage[14].

Our findings demonstrate that *Cxxc1*-deficient T_{reg} cells exhibit reduced H3K4me3 levels at T_{reg}-specific loci, indicating that CXXC1 plays a critical role in regulating this epigenetic modification. This is consistent with previous studies showing that CXXC1 acts as a non-catalytic component of

the Set1/COMPASS complex [65–68], which includes the H3K4 methyltransferases SETD1A and SETD1B, the primary enzymes responsible for H3K4 trimethylation. Given this, we propose that CXXC1 supports H3K4me3 deposition in T_{reg} cells by interacting with and stabilizing the activity of the Set1/COMPASS complex. Further studies are required to directly investigate the interactions between CXXC1 and these methyltransferases in the T_{reg} cell context.

Our results offer provide novel insights into the suppressive functions, heterogeneity, and regulatory mechanisms of T_{reg} cells. Maintaining T_{reg} cell homeostasis and function remains a challenge in harnessing T_{reg} cells for the treatment of autoimmune diseases and the prevention of graft rejection.

Acknowledgements

We thank B. Li (Shanghai Jiao Tong University School of Medicine, Shanghai, China) for providing *Foxp3*$^{YFP\text{-}Cre}$ mice, X.Y. Zhou(Chinese Academy of Science (CAS), Beijing, China) for providing the FOXP3 CUT&Tag antibody, and X. L. Liu (Shanghai Institutes for Biological Sciences, Chinese Academy of Sciences) for his generous gifts of cell lines. We thank Y. Huang, Y. Li, J. Wan, C.Guo, and Z. Lin from the Core Facilities, Zhejiang University School of Medicine for their technical support and S. Hong, Y. Ding, H. Jin, Q. Wang, and X. Zhang from Animal Facilities, Zhejiang University, for feeding the mice.

Additional information

Funding

This work was supported by grants from the National Natural Science Foundation of China (32341002, 32030035, 32321002, 32100693, and 32270839), the National Key R & D Program of China (2023YFA1800202, 2024YFF0728703, 2022YFA1103702, 2022YFA1103200), the Zhejiang Provincial Natural Science Foundation of China (LZ21C080001, LZ23C070003), Science and Technology Innovation 2030-Major Project (2021ZD0200405), Key project of the Experimental Technology Program of Zhejiang University (SZD202203), and the Fundamental Research Funds for the Central Universities (226-2024-00161).

Author contributions

L.W. and L.S.: supervision, conceptualization, project administration, and writing—review and editing. L.W., L.S. and X.M: funding acquisition. X.M: investigation, methodology, project administration, and writing— original draft. Y.Z.and K.L.: bioinformatics analysis. Y. W., X.L., J.C., C.L., Y.Z., S.W., S.T., Q.X., L.D., X.S., and X.G.: investigation and methodology.

Additional files

Supplemental information

Supplementary Table 3

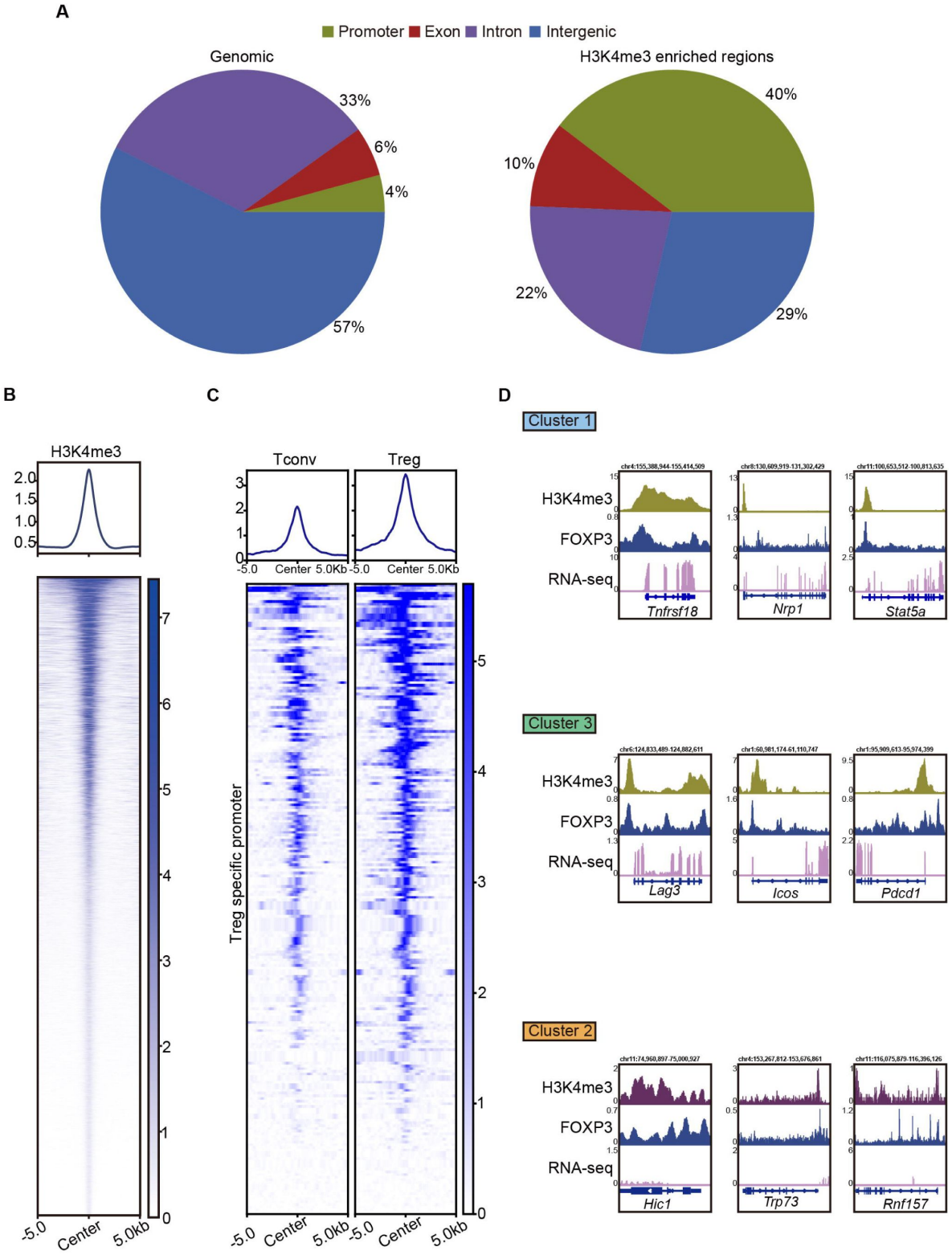

Supplementary Figure 1

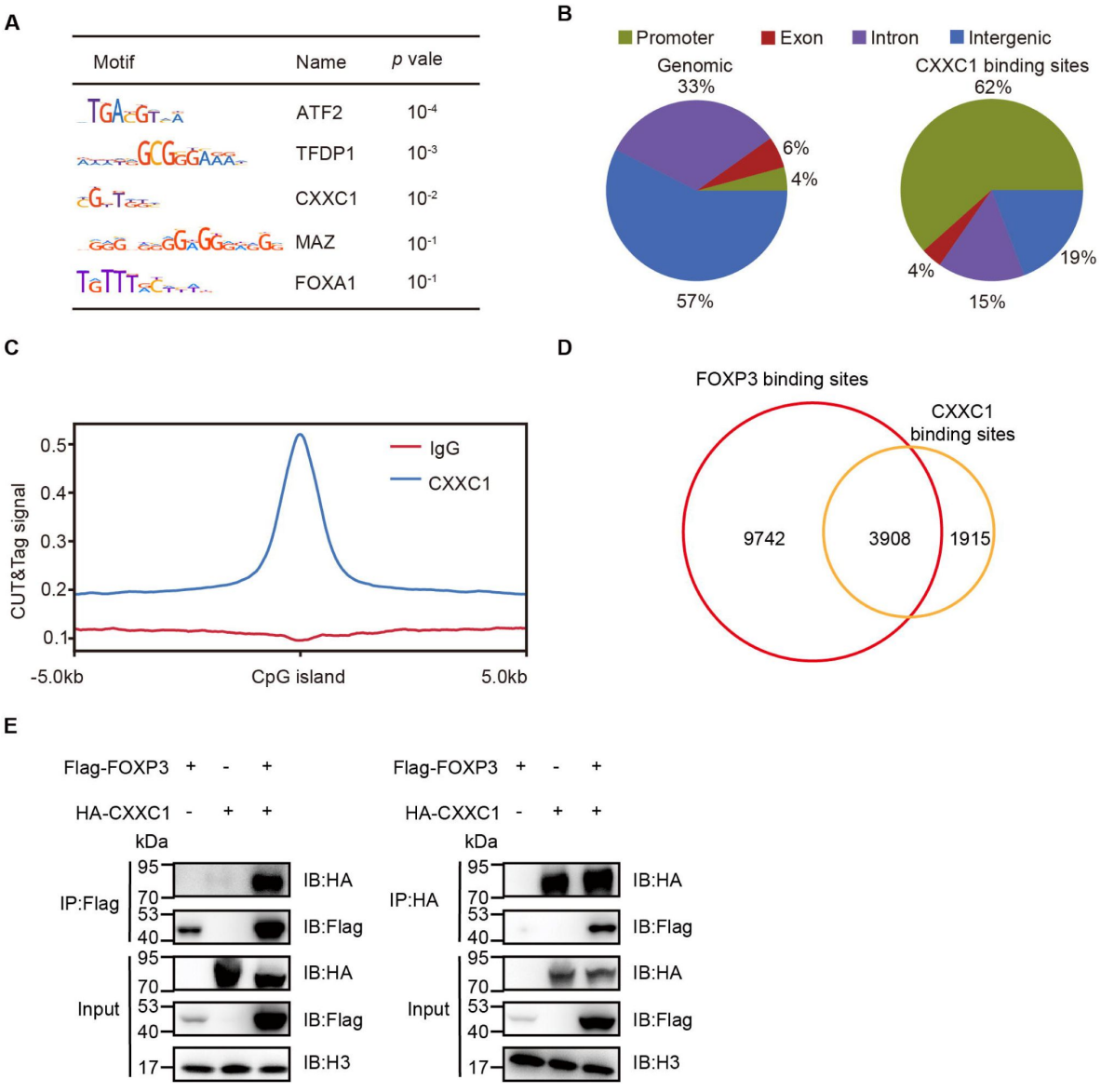

Supplementary Figure 2

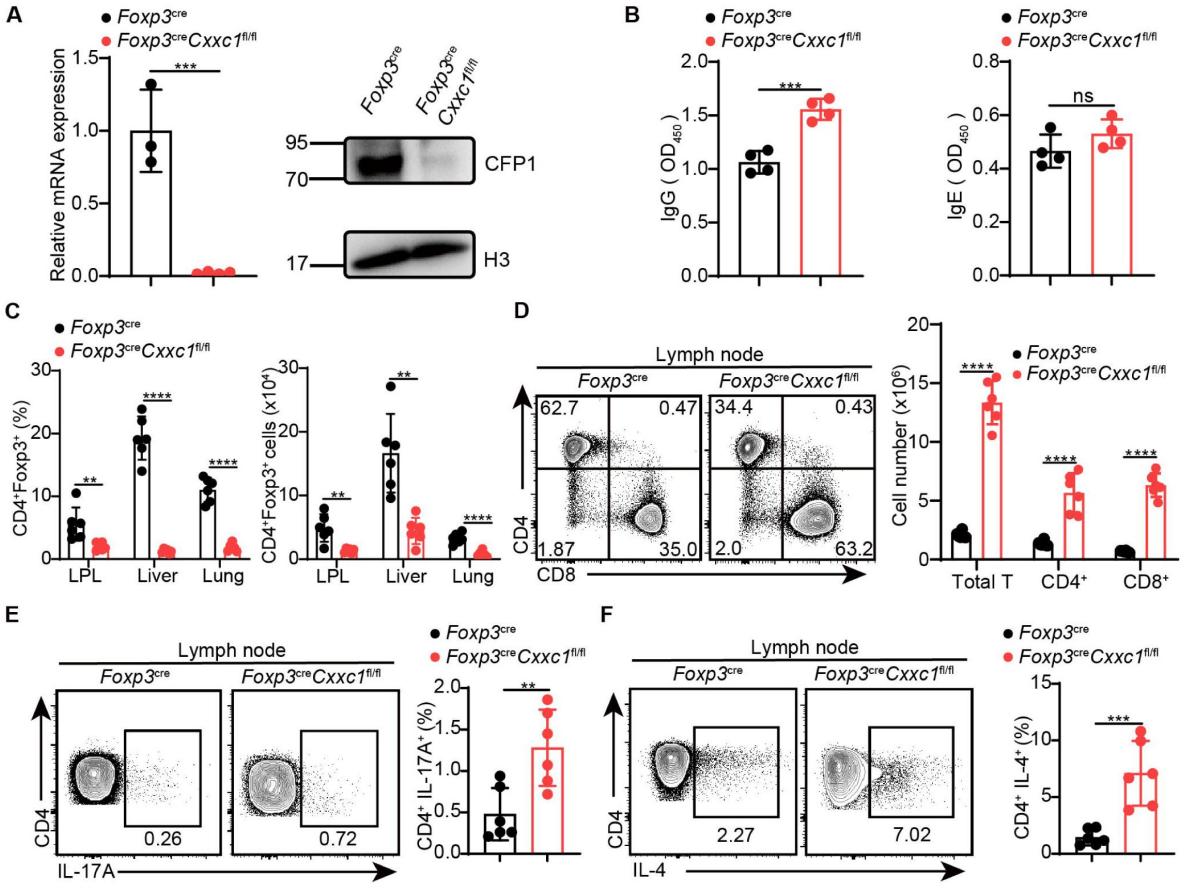

Supplementary Figure 3

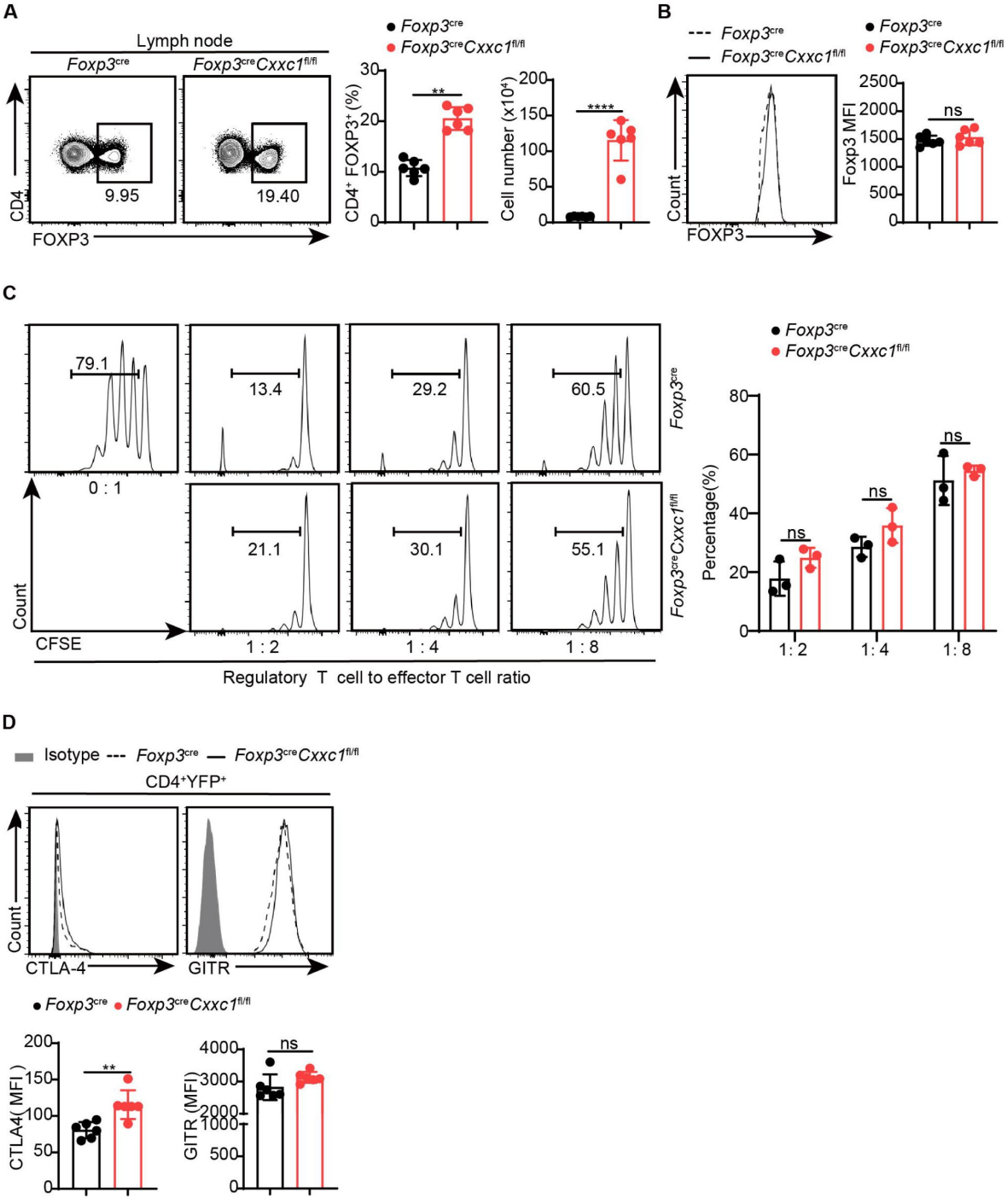

Supplementary Figure 4

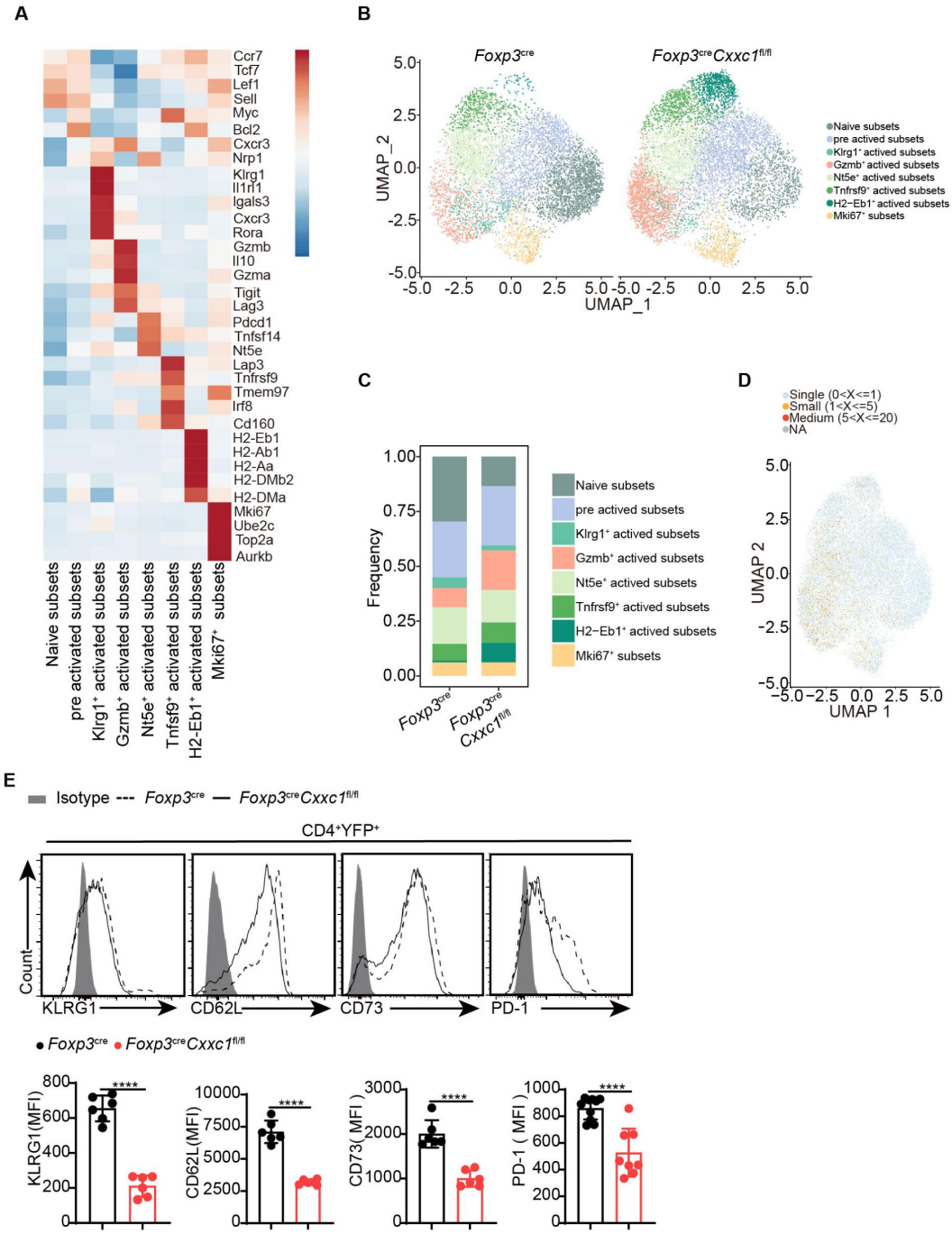

Supplementary Figure 5

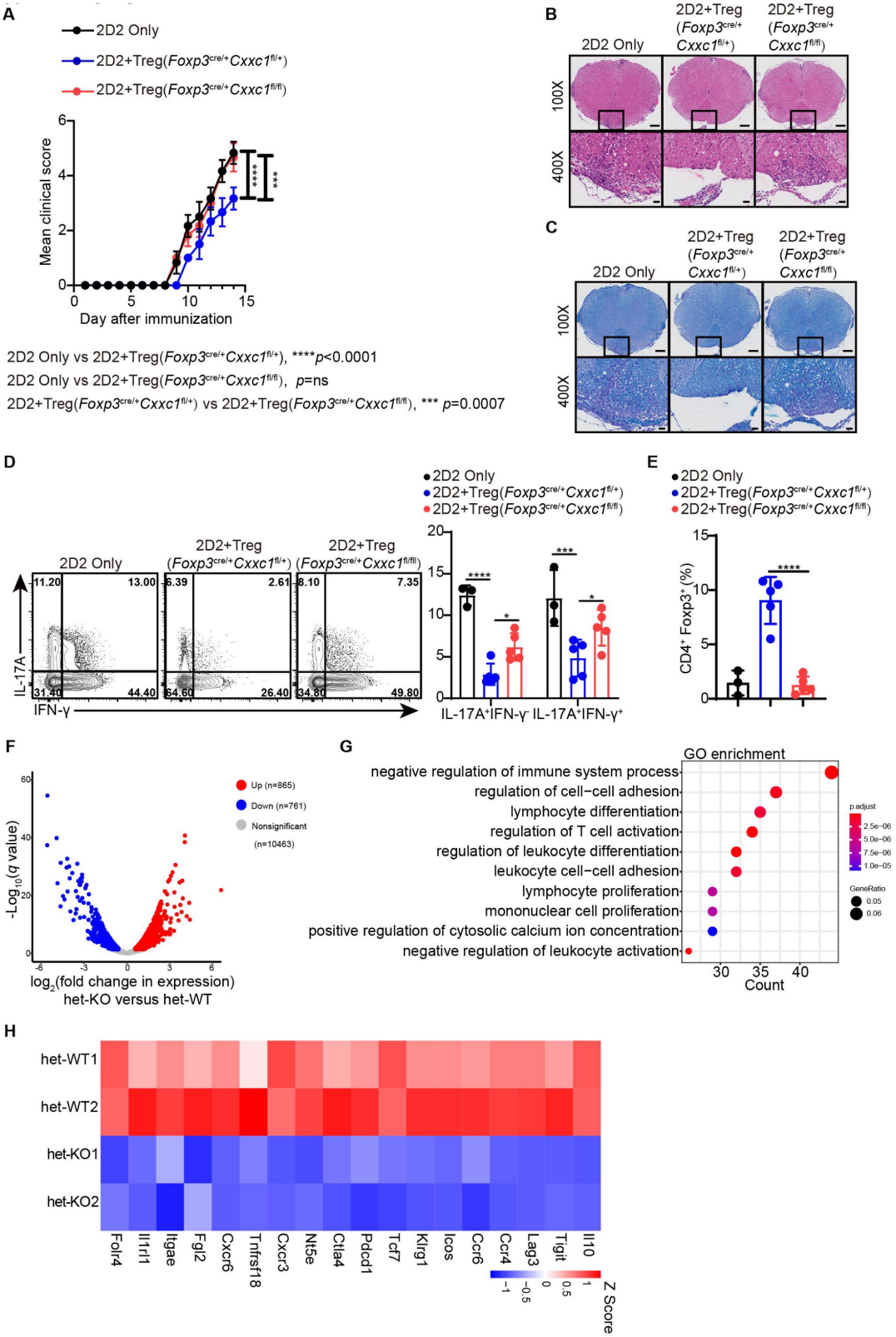

Supplementary Figure 6

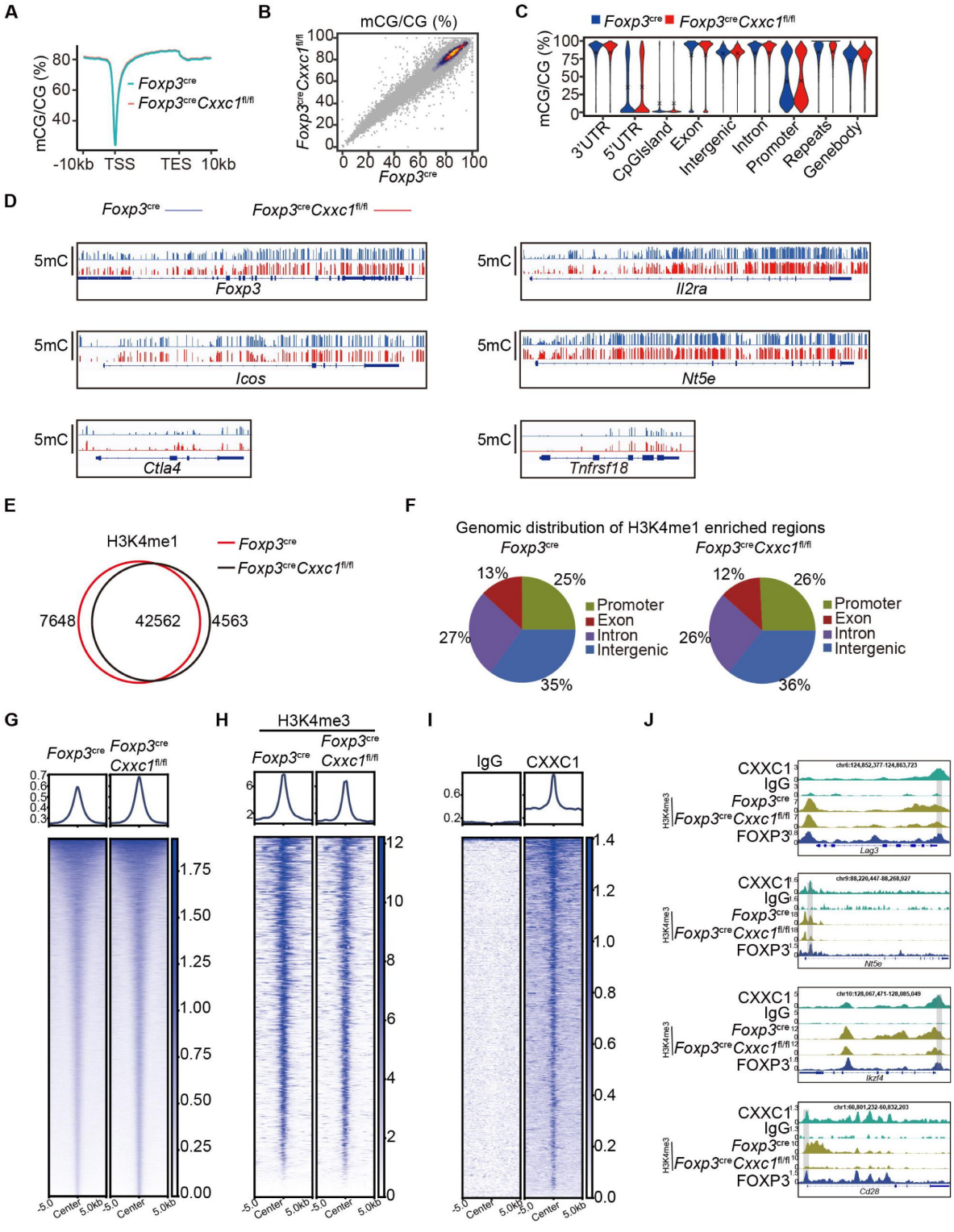

Supplementary Figure 7

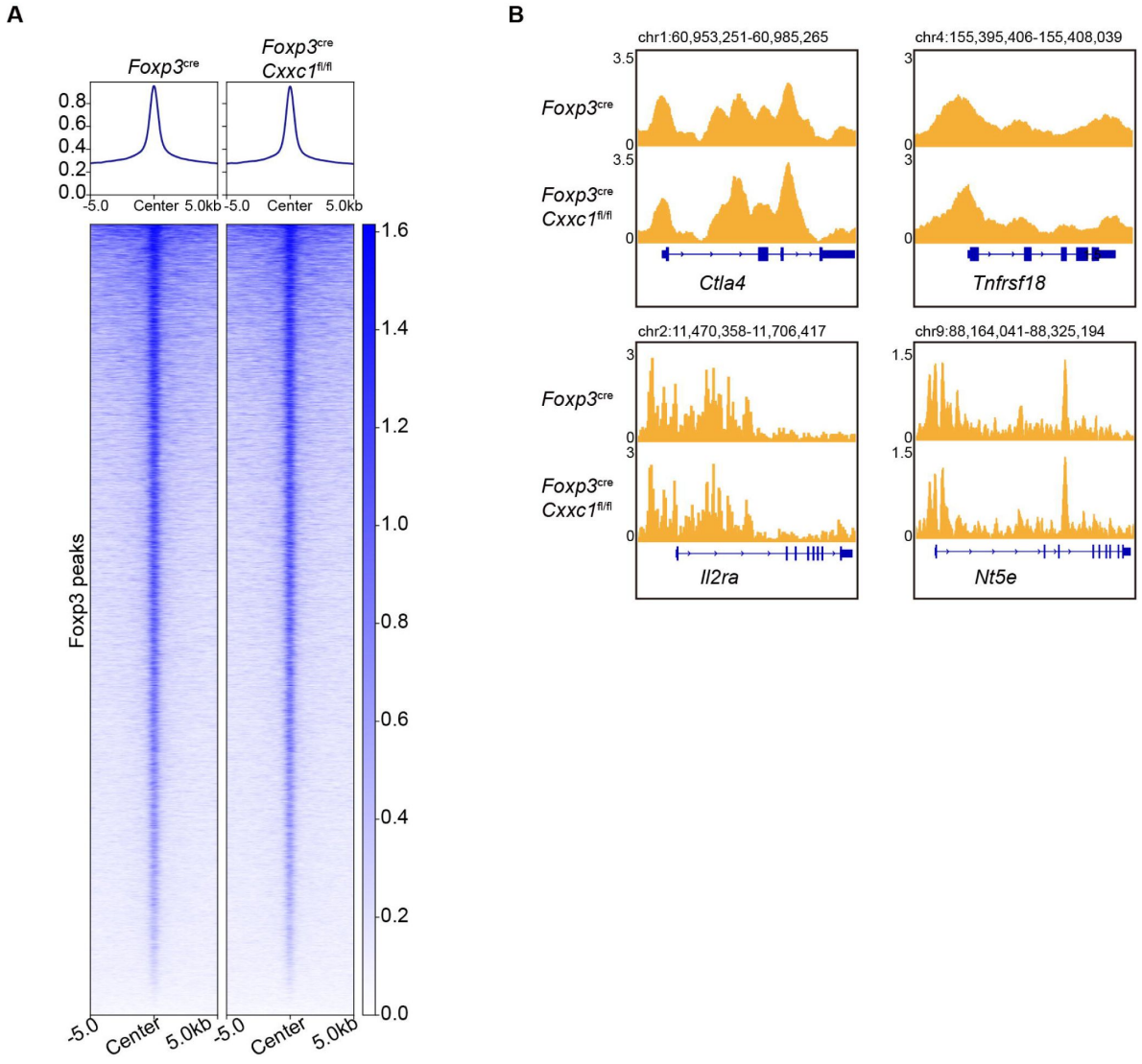

Supplementary Figure 8

References

1 Sakaguchi S., Yamaguchi T., Nomura T., Ono M. 2008) **Regulatory T cells and immune tolerance** *Cell* **133**:775–787 https://doi.org/10.1016/j.cell.2008.05.009

2 Josefowicz S. Z., Lu L. F., Rudensky A. Y. 2012) **Regulatory T Cells: Mechanisms of Differentiation and Function** *Annual Review of Immunology* **30**:531–564

3 Singer B. D., King L. S., D'Alessio F. R 2014) **Regulatory T cells as immunotherapy** *Frontiers in Immunology* **5** https://doi.org/10.3389/fimmu.2014.00046

4 Ohkura N., Sakaguchi S 2020) **Transcriptional and epigenetic basis of Treg cell development and function: its genetic anomalies or variations in autoimmune diseases** *Cell Research* **30**:465–474 https://doi.org/10.1038/s41422-020-0324-7

5 Littman D. R., Rudensky A. Y 2010) **Th17 and Regulatory T Cells in Mediating and Restraining Inflammation** *Cell* **140**:845–858 https://doi.org/10.1016/j.cell.2010.02.021

6 Sakaguchi S., Vignali D. A. A., Rudensky A. Y., Niec R. E., Waldmann H 2013) **The plasticity and stability of regulatory T cells** *Nature Reviews Immunology* **13**:461–467 https://doi.org/10.1038/nri3464

7 Fontenot J. D., Gavin M. A., Rudensky A. Y 2003) **Foxp3 programs the development and function of CD4+CD25+ regulatory T cells** *Nat Immunol* **4**:330–336 https://doi.org/10.1038/ni904

8 Van Gool F., Nguyen M. L. T., Mumbach M. R., Satpathy A. T., Rosenthal W. L., Giacometti S., Le D. T., Liu W., Brusko T. M., Anderson M. S., Rudensky A. Y., Marson A., Chang H. Y., Bluestone J. A 2019) **A Mutation in the Transcription Factor Foxp3 Drives T Helper 2 Effector Function in Regulatory T Cells** *Immunity* **50**:362 https://doi.org/10.1016/j.immuni.2018.12.016

9 Katoh H., Qin Z. S., Liu R., Wang L., Li W., Li X., Wu L., Du Z., Lyons R., Liu C.-G., Liu X., Dou Y., Zheng P., Liu Y 2011) **FOXP3 Orchestrates H4K16 Acetylation and H3K4 Trimethylation for Activation of Multiple Genes by Recruiting MOF and Causing Displacement of PLU-1** *Molecular Cell* **44**:770–784 https://doi.org/10.1016/j.molcel.2011.10.012

10 Wang L., Liu Y., Han R., Beier U. H., Bhatti T. R., Akimova T., Greene M. I., Hiebert S. W., Hancock W. W 2015) **FOXP3(+) regulatory T cell development and function require histone/protein deacetylase 3** *Journal of Clinical Investigation* **125**:1111–1123 https://doi.org/10.1172/jci77088

11 Arvey A., van der Veeken J., Samstein R. M., Feng Y., Stamatoyannopoulos J. A., Rudensky A. Y 2014) **Inflammation-induced repression of chromatin bound by the transcription factor Foxp3 in regulatory T cells** *Nature Immunology* **15**:580–587 https://doi.org/10.1038/ni.2868

12 Ruthenburg A. J., Allis C. D., Wysocka J 2007) **Methylation of lysine 4 on histone H3: Intricacy of writing and reading a single epigenetic mark** *Molecular Cell* **25**:15–30 https://doi.org/10.1016/j.molcel.2006.12.014

13 Takahashi Y.-h., Westfield G. H., Oleskie A. N., Trievel R. C., Shilatifard A., Skiniotis G. 2011) **Structural analysis of the core COMPASS family of histone H3K4 methylases from yeast to**

human *Proceedings of the National Academy of Sciences of the United States of America* **108**:20526–20531 https://doi.org/10.1073/pnas.1109360108

14 Wang T., Guo J., Li L., Jin Q., Zhang F., Hou B., Zhang Y., Zhou X 2024) **The histone lysine methyltransferase MLL1 regulates the activation and functional specialization of regulatory T cells** *Cell Reports* **43** https://doi.org/10.1016/j.celrep.2024.114222

15 Placek K., Hu G., Cui K., Zhang D., Ding Y., Lee J.-E., Jang Y., Wang C., Konkel J. E., Song J., Liu C., Ge K., Chen W., Zhao K 2017) **MLL4 prepares the enhancer landscape for Foxp3 induction via chromatin looping** *Nature Immunology* **18**:1035 https://doi.org/10.1038/ni.3812

16 Yang Y., Yang Y., Chan K., Couture J.-F 2021) **Analyzing the impact of CFP1 mutational landscape on epigenetic signaling** *Faseb Journal* **35** https://doi.org/10.1096/fj.202100427R

17 Tate C. M., Lee J.-H., Skalnik D. G 2010) **CXXC finger protein 1 restricts the Setd1A histone H3K4 methyltransferase complex to euchromatin** *Febs Journal* **277**:210–223 https://doi.org/10.1111/j.1742-4658.2009.07475.x

18 Cao W., Guo J., Wen X., Miao L., Lin F., Xu G., Ma R., Yin S., Hui Z., Chen T., Guo S., Chen W., Huang Y., Liu Y., Wang J., Wei L., Wang L 2016) **CXXC finger protein 1 is critical for T-cell intrathymic development through regulating H3K4 trimethylation** *Nat Commun* **7** https://doi.org/10.1038/ncomms11687

19 Hui Z., Zhou L., Xue Z., Zhou L., Luo Y., Lin F., Liu X., Hong S., Li W., Wang D., Lu L., Wang J., Wang L 2018) **Cxxc Finger Protein 1 Positively Regulates GM-CSF-Derived Macrophage Phagocytosis Through Csf2rα-Mediated Signaling** *Frontiers in Immunology* **9** https://doi.org/10.3389/fimmu.2018.01885

20 Lin F., Meng X., Guo Y., Cao W., Liu W., Xia Q., Hui Z., Chen J., Hong S., Zhang X., Wu C., Wang D., Wang J., Lu L., Qian W., Wei L., Wang L 2019) **Epigenetic initiation of the T(H)17 differentiation program is promoted by Cxxc finger protein 1** *Science Advances* **5** https://doi.org/10.1126/sciadv.aax1608

21 Shen X., Gao X., Luo Y., Xu Q., Fan Y., Hong S., Huang Z., Liu X., Wang Q., Chen Z., Wang D., Lu L., Wu C., Liang H., Wang L 2023) **Cxxc finger protein 1 maintains homeostasis and function of intestinal group 3 innate lymphoid cells with aging** *Nature Aging* **3**:965 https://doi.org/10.1038/s43587-023-00453-7

22 Cao W., Guo J., Wen X., Miao L., Lin F., Xu G., Ma R., Yin S., Hui Z., Chen T., Guo S., Chen W., Huang Y., Liu Y., Wang J., Wei L., Wang L 2016) **CXXC finger protein 1 is critical for T-cell intrathymic development through regulating H3K4 trimethylation** *Nature Communications* **7** https://doi.org/10.1038/ncomms11687

23 Zhou L., Wang S., Hu W., Liu X., Xu L., Tong B., Zhang T., Xue Z., Guo Y., Zhao J., Lu L., Fan H., Qian W., Chen J., Chen W., Wang L 2023) **T cell proliferation requires ribosomal maturation in nucleolar condensates dependent on DCAF13** *Journal of Cell Biology* **222** https://doi.org/10.1083/jcb.202201096

24 Chou W.-C., Guo Z., Guo H., Chen L., Zhang G., Liang K., Xie L., Tan X., Gibson S. A., Rampanelli E., Wang Y., Montgomery S. A., Brickey W. J., Deng M., Freeman L., Zhang S., Su M. A., Chen X., Wan Y. Y., Ting J. P. Y 2021) **AIM2 in regulatory T cells restrains autoimmune diseases** *Nature* **591**:300 https://doi.org/10.1038/s41586-021-03231-w

25 Zeng H., Yang K., Cloer C., Neale G., Vogel P., Chi H 2013) **mTORC1 couples immune signals and metabolic programming to establish T(reg)-cell function** *Nature* **499**:485–490 https://doi.org/10.1038/nature12297

26 Lu D., Liu L., Sun Y., Song J., Yin Q., Zhang G., Qi F., Hu Z., Yang Z., Zhou Z., Hu Y., Zhang L., Ji J., Zhao X., Jin Y., McNutt M. A., Yin Y 2020) **The phosphatase PAC1 acts as a T cell suppressor and attenuates host antitumor immunity** *Nature Immunology* **21**:287 https://doi.org/10.1038/s41590-019-0577-9

27 Chen J., Liu K., Luo Y., Kang M., Wang J., Chen G., Qi J., Wu W., Wang B., Han Y., Shi L., Wang K., Han X., Ma X., Liu W., Ding Y., Wang L., Liang H., Wang L., Chen J 2023) **Single-Cell Profiling of Tumor Immune Microenvironment Reveals Immune Irresponsiveness in Gastric Signet-Ring Cell Carcinoma** *Gastroenterology* **165**:88–103 https://doi.org/10.1053/j.gastro.2023.03.008

28 Marson A., Kretschmer K., Frampton G. M., Jacobsen E. S., Polansky J. K., Maclsaac K. D., Levine S. S., Fraenkel E., von Boehmer H., Young R. A 2007) **Foxp3 occupancy and regulation of key target genes during T-cell stimulation** *Nature* **445**:931–935 https://doi.org/10.1038/nature05478

29 Zheng Y., Josefowicz S. Z., Kas A., Chu T.-T., Gavin M. A., Rudensky A. Y 2007) **Genome-wide analysis of Foxp3 target genes in developing and mature regulatory T cells** *Nature* **445**:936–940 https://doi.org/10.1038/nature05563

30 Ono M., Yaguchi H., Ohkura N., Kitabayashi I., Nagamura Y., Nomura T., Miyachi Y., Tsukada T., Sakaguchi S 2007) **Foxp3 controls regulatory T-cell function by interacting with AML1/Runx1** *Nature* **446**:685–689 https://doi.org/10.1038/nature05673

31 Fu W., Ergun A., Lu T., Hill J. A., Haxhinasto S., Fassett M. S., Gazit R., Adoro S., Glimcher L., Chan S., Kastner P., Rossi D., Collins J. J., Mathis D., Benoist C 2012) **A multiply redundant genetic switch 'locks in' the transcriptional signature of regulatory T cells** *Nature Immunology* **13**:972–980 https://doi.org/10.1038/ni.2420

32 Ohkura N., Hamaguchi M., Morikawa H., Sugimura K., Tanaka A., Ito Y., Osaki M., Tanaka Y., Yamashita R., Nakano N., Huehn J., Fehling H. J., Sparwasser T., Nakai K., Sakaguchi S 2012) **T Cell Receptor Stimulation-Induced Epigenetic Changes and Foxp3 Expression Are Independent and Complementary Events Required for Treg Cell Development** *Immunity* **37**:785–799 https://doi.org/10.1016/j.immuni.2012.09.010

33 Wei G., Wei L., Zhu J., Zang C., Hu-Li J., Yao Z., Cui K., Kanno Y., Roh T.-Y., Watford W. T., Schones D. E., Peng W., Sun H.-w., Paul W. E., O'Shea J. J., Zhao K. 2009) **Global Mapping of H3K4me3 and H3K27me3 Reveals Specificity and Plasticity in Lineage Fate Determination of Differentiating CD4(+) T Cells** *Immunity* **30**:155–167 https://doi.org/10.1016/j.immuni.2008.12.009

34 Konopacki C., Pritykin Y., Rubtsov Y., Leslie C. S., Rudensky A. Y 2019) **Transcription factor Foxp1 regulates Foxp3 chromatin binding and coordinates regulatory T cell function** *Nature Immunology* **20**:232 https://doi.org/10.1038/s41590-018-0291-z

35 Hill J. A., Feuerer M., Tash K., Haxhinasto S., Perez J., Melamed R., Mathis D., Benoist C 2007) **Foxp3 transcription-factor-dependent and -independent regulation of the regulatory T cell transcriptional signature** *Immunity* **27**:786–800 https://doi.org/10.1016/j.immuni.2007.09.010

36 Oh H., Grinberg-Bleyer Y., Liao W., Maloney D., Wang P., Wu Z., Wang J., Bhatt D. M., Heise N., Schmid R. M., Hayden M. S., Klein U., Rabadan R., Ghosh S 2017) **An NF-kappaB Transcription-Factor-Dependent Lineage-Specific Transcriptional Program Promotes Regulatory T Cell Identity and Function** *Immunity* **47**:450–465 https://doi.org/10.1016/j.immuni.2017.08.010

37 Rubtsov Y. P., Rasmussen J. P., Chi E. Y., Fontenot J., Castelli L., Ye X., Treuting P., Siewe L., Roers A., Henderson W. R., Muller W., Rudensky A. Y 2008) **Regulatory T cell-derived interleukin-10 limits inflammation at environmental interfaces** *Immunity* **28**:546–558 https://doi.org/10.1016/j.immuni.2008.02.017

38 Fontenot J. D., Gavin M. A., Rudensky A. Y 2003) **Foxp3 programs the development and function of CD4(+)CD25(+) regulatory T cells** *Nature Immunology* **4**:330–336 https://doi.org/10.1038/ni904

39 Kim J. M., Rasmussen J. P., Rudensky A. Y 2007) **Regulatory T cells prevent catastrophic autoimmunity throughout the lifespan of mice** *Nature Immunology* **8**:191–197 https://doi.org/10.1038/ni1428

40 Shevyrev D., Tereshchenko V. 2020) **Treg Heterogeneity, Function, and Homeostasis** *Frontiers in Immunology* **10** https://doi.org/10.3389/fimmu.2019.03100

41 Zagorulya M., Yim L., Morgan D. M., Edwards A., Torres-Mejia E., Momin N., McCreery C. V., Zamora I. L., Horton B. L., Fox J. G., Wittrup K. D., Love J. C., Spranger S 2023) **Tissue-specific abundance of interferon-gamma drives regulatory T cells to restrain DC1-mediated priming of cytotoxic T cells against lung cancer** *Immunity* **56**:386 https://doi.org/10.1016/j.immuni.2023.01.010

42 Dikiy S., Rudensky A. Y 2023) **Principles of regulatory T cell function** *Immunity* **56**:240–255 https://doi.org/10.1016/j.immuni.2023.01.004

43 Street K., Risso D., Fletcher R. B., Das D., Ngai J., Yosef N., Purdom E., Dudoit S 2018) **Slingshot: cell lineage and pseudotime inference for single-cell transcriptomics** *Bmc Genomics* **19** https://doi.org/10.1186/s12864-018-4772-0

44 Tarbell K. V., Yamazaki S., Olson K., Toy P., Steinman R. M 2004) **CD25+CD4+T cells, expanded with dendritic cells presenting a single autoantigenic peptide, suppress autoimmune diabetes** *Journal of Experimental Medicine* **199**:1467–1477 https://doi.org/10.1084/jem.20040180

45 Hori S., Haury M., Coutinho A., Demengeot J 2002) **Specificity requirements for selection and effector functions of CD25+4+ regulatory T cells in anti-myelin basic protein T cell receptor transgenic mice** *Proceedings of the National Academy of Sciences of the United States of America* **99**:8213–8218 https://doi.org/10.1073/pnas.122224799

46 Butler J. S., Lee J.-H., Skalnik D. G 2008) **CFP1 Interacts with DNMT1 Independently of Association with the Setd1 Histone H3K4 Methyltransferase Complexes** *DNA and Cell Biology* **27**:533–543 https://doi.org/10.1089/dna.2007.0714

47 Butler J. S., Palam L. R., Tate C. M., Sanford J. R., Wek R. C., Skalnik D. G 2009) **DNA Methyltransferase Protein Synthesis Is Reduced in CXXC Finger Protein 1-Deficient Embryonic Stem Cells** *DNA and Cell Biology* **28**:223–231 https://doi.org/10.1089/dna.2009.0854

48 Benayoun B. A., Pollina E. A., Ucar D., Mahmoudi S., Karra K., Wong E. D., Devarajan K., Daugherty A. C., Kundaje A. B., Mancini E., Hitz B. C., Gupta R., Rando T. A., Baker J. C., Snyder

M. P., Cherry J. M., Brunet A 2014) **H3K4me3 Breadth Is Linked to Cell Identity and Transcriptional Consistency** *Cell* **158**:673–688 https://doi.org/10.1016/j.cell.2014.06.027

49 Zacarias-Cabeza J., Belhocine M., Vanhille L., Cauchy P., Koch F., Pekowska A., Fenouil R., Bergon A., Gut M., Gut I., Eick D., Imbert J., Ferrier P., Andrau J.-C., Spicuglia S 2015) **Transcription-Dependent Generation of a Specialized Chromatin Structure at the TCRβ Locus** *Journal of Immunology* **194**:3432–3443 https://doi.org/10.4049/jimmunol.1400789

50 Chen K., Chen Z., Wu D., Zhang L., Lin X., Su J., Rodriguez B., Xi Y., Xia Z., Chen X., Shi X., Wang Q., Li W 2015) **Broad H3K4me3 is associated with increased transcription elongation and enhancer activity at tumor-suppressor genes** *Nature Genetics* **47**:1149 https://doi.org/10.1038/ng.3385

51 Zhang R., Huynh A., Whitcher G., Chang J., Maltzman J. S., Turka L. A 2013) **An obligate cell-intrinsic function for CD28 in Tregs** *Journal of Clinical Investigation* **123**:580–593 https://doi.org/10.1172/jci65013

52 Gokhale A. S., Gangaplara A., Lopez-Occasio M., Thornton A. M., Shevach E. M 2019) **Selective deletion of Eos (Ikzf4) in T-regulatory cells leads to loss of suppressive function and development of systemic autoimmunity** *Journal of Autoimmunity* **105** https://doi.org/10.1016/j.jaut.2019.06.011

53 Wan Y. Y., Flavell R. A 2007) **Regulatory T-cell functions are subverted and converted owing to attenuated Foxp3 expression** *Nature* **445**:766–770 https://doi.org/10.1038/nature05479

54 Chen C., Rowell E. A., Thomas R. M., Hancock W. W., Wells A. D 2006) **Transcriptional regulation by Foxp3 is associated with direct promoter occupancy and modulation of histone acetylation** *Journal of Biological Chemistry* **281**:36828–36834 https://doi.org/10.1074/jbc.M608848200

55 Morikawa H., Ohkura N., Vandenbon A., Itoh M., Nagao-Sato S., Kawaji H., Lassmann T., Carninci P., Hayashizaki Y., Forrest A. R. R., Standley D. M., Date H., Sakaguchi S., Consortium F 2014) **Differential roles of epigenetic changes and Foxp3 expression in regulatory T cell-specific transcriptional regulation** *Proceedings of the National Academy of Sciences of the United States of America* **111**:5289–5294 https://doi.org/10.1073/pnas.1312717110

56 Pan F., Yu H., Dang E. V., Barbi J., Pan X., Grosso J. F., Jinasena D., Sharma S. M., McCadden E. M., Getnet D., Drake C. G., Liu J. O., Ostrowski M. C., Pardoll D. M 2009) **Eos Mediates Foxp3-Dependent Gene Silencing in CD4+ Regulatory T Cells** *Science* **325**:1142–1146 https://doi.org/10.1126/science.1176077

57 DuPage M., Chopra G., Quiros J., Rosenthal W. L., Morar M. M., Holohan D., Zhang R., Turka L., Marson A., Bluestone J. A 2015) **The Chromatin-Modifying Enzyme Ezh2 Is Critical for the Maintenance of Regulatory T Cell Identity after Activation** *Immunity* **42**:227–238 https://doi.org/10.1016/j.immuni.2015.01.007

58 Liu X., Wang C., Liu W., Li J., Li C., Kou X., Chen J., Zhao Y., Gao H., Wang H., Zhang Y., Gao Y., Gao S 2016) **Distinct features of H3K4me3 and H3K27me3 chromatin domains in pre-implantation embryos** *Nature* **537**:558 https://doi.org/10.1038/nature19362

59 Sze C. C., Ozark P. A., Cao K., Ugarenko M., Das S., Wang L., Marshall S. A., Rendleman E. J., Ryan C. A., Zha D., Douillet D., Chen F. X., Shilatifard A 2020) **Coordinated regulation of cellular identity-associated H3K4me3 breadth by the COMPASS family** *Science Advances* **6** https://doi.org/10.1126/sciadv.aaz4764

60 Dahl J. A., Jung I., Aanes H., Greggains G. D., Manaf A., Lerdrup M., Li G., Kuan S., Li B., Lee A. Y., Preissl S., Jermstad I., Haugen M. H., Suganthan R., Bjoras M., Hansen K., Dalen K. T., Fedorcsak P., Ren B., Klungland A 2016) **Broad histone H3K4me3 domains in mouse oocytes modulate maternal-to-zygotic transition** *Nature* **537**:548 https://doi.org/10.1038/nature19360

61 Zhang B., Zheng H., Huang B., Li W., Xiang Y., Peng X., Ming J., Wu X., Zhang Y., Xu Q., Liu W., Kou X., Zhao Y., He W., Li C., Chen B., Li Y., Wang Q., Ma J., Yin Q., Kee K., Meng A., Gao S., Xu F., Na J., Xie W 2016) **Allelic reprogramming of the histone modification H3K4me3 in early mammalian development** *Nature* **537**:553 https://doi.org/10.1038/nature19361

62 Zhang Z., Shi L., Dawany N., Kelsen J., Petri M. A., Sullivan K. E 2016) **H3K4 tri-methylation breadth at transcription start sites impacts the transcriptome of systemic lupus erythematosus** *Clinical Epigenetics* **8** https://doi.org/10.1186/s13148-016-0179-4

63 Wong S. H. K., Goode D. L., Iwasaki M., Wei M. C., Kuo H.-P., Zhu L., Schneidawind D., Duque-Afonso J., Weng Z., Cleary M. L 2015) **The H3K4-Methyl Epigenome Regulates Leukemia Stem Cell Oncogenic Potential** *Cancer Cell* **28**:198–209 https://doi.org/10.1016/j.ccell.2015.06.003

64 Deaglio S., Dwyer K. M., Gao W., Friedman D., Usheva A., Erat A., Chen J.-F., Enjyoji K., Linden J., Oukka M., Kuchroo V. K., Strom T. B., Robson S. C 2007) **Adenosine generation catalyzed by CD39 and CD73 expressed on regulatory T cells mediates immune suppression** *Journal of Experimental Medicine* **204**:1257–1265 https://doi.org/10.1084/jem.20062512

65 Lee J. H., Skalnik D. G 2005) **CpG-binding protein (CXXC finger protein 1) is a component of the mammalian set1 histone H3-Lys4 methyltransferase complex, the analogue of the yeast Set1/COMPASS complex** *Journal of Biological Chemistry* **280**:41725–41731 https://doi.org/10.1074/jbc.M508312200

66 Thomson J. P., Skene P. J., Selfridge J., Clouaire T., Guy J., Webb S., Kerr A. R. W., Deaton A., Andrews R., James K. D., Turner D. J., Illingworth R., Bird A 2010) **CpG islands influence chromatin structure via the CpG-binding protein Cfp1** *Nature* **464**:1082–U1162 https://doi.org/10.1038/nature08924

67 Shilatifard A. 2012) **The COMPASS family of histone H3K4 methylases: mechanisms of regulation in development and disease pathogenesis** *Annual Review of Biochemistry* **81**:65–95

68 Brown D. A., Di Cerbo V., Feldmann A., Ahn J., Ito S., Blackledge N. P., Nakayama M., McClellan M., Dimitrova E., Turberfield A. H., Long H. K., King H. W., Kriaucionis S., Schermelleh L., Kutateladze T. G., Koseki H., Klose R. J 2017) **The SET1 Complex Selects Actively Transcribed Target Genes via Multivalent Interaction with CpG Island Chromatin** *Cell Reports* **20**:2313–2327 https://doi.org/10.1016/j.celrep.2017.08.030

Author information

Xiaoyu Meng[†]

Institute of Immunology and Bone Marrow Transplantation Center, The First Affiliated Hospital, Zhejiang University School of Medicine, Hangzhou, China, Zhejiang University School of Medicine, Hangzhou, China, Liangzhu Laboratory, Zhejiang University Medical Center, Hangzhou, China

†These authors contributed equally to this work.

Yezhang Zhu[†]
Department of Hematology, Tongji Hospital, School of Medicine, Tongji University, Shanghai, China, Shanghai Key Laboratory of Signaling and Disease Research, Frontier Science Center of Stem Cell Research, National Stem Cell Translational Resource Center, School of Life Sciences and Technology, Tongji University, Shanghai, China

†These authors contributed equally to this work.

Kuai Liu[†]
Institute of Immunology and Bone Marrow Transplantation Center, The First Affiliated Hospital, Zhejiang University School of Medicine, Hangzhou, China, Zhejiang University School of Medicine, Hangzhou, China, Liangzhu Laboratory, Zhejiang University Medical Center, Hangzhou, China

†These authors contributed equally to this work.

Yuxi Wang
Laboratory Animal Center, Zhejiang University, Hangzhou, China

Xiaoqian Liu
Institute of Immunology and Bone Marrow Transplantation Center, The First Affiliated Hospital, Zhejiang University School of Medicine, Hangzhou, China, Zhejiang University School of Medicine, Hangzhou, China, Liangzhu Laboratory, Zhejiang University Medical Center, Hangzhou, China

Chenxin Liu
Zhejiang University School of Medicine, Hangzhou, China

Yan Zeng
Institute of Immunology and Bone Marrow Transplantation Center, The First Affiliated Hospital, Zhejiang University School of Medicine, Hangzhou, China, Zhejiang University School of Medicine, Hangzhou, China, Liangzhu Laboratory, Zhejiang University Medical Center, Hangzhou, China

Shuai Wang
Institute of Immunology and Bone Marrow Transplantation Center, The First Affiliated Hospital, Zhejiang University School of Medicine, Hangzhou, China, Zhejiang University School of Medicine, Hangzhou, China, Liangzhu Laboratory, Zhejiang University Medical Center, Hangzhou, China

Xianzhi Gao
Institute of Immunology and Bone Marrow Transplantation Center, The First Affiliated Hospital, Zhejiang University School of Medicine, Hangzhou, China, Zhejiang University School of Medicine, Hangzhou, China, Liangzhu Laboratory, Zhejiang University Medical Center, Hangzhou, China

Xin Shen
Co-Facility Center, Zhejiang University School of Medicine, Hangzhou, China

Jing Chen
Department of Gastrointestinal Surgery, The Second Affiliated Hospital, Zhejiang University School of Medicine, Hangzhou, China

Sijue Tao
Laboratory Animal Center, Zhejiang University, Hangzhou, China

Qianying Xu
Zhejiang University School of Medicine, Hangzhou, China

Linjia Dong
School of Basic Medical Sciences and Forensic Medicine, Hangzhou Medical College, Hangzhou, China

Li Shen
MOE Key Laboratory of Biosystems Homeostasis & Protection and Zhejiang Provincial Key Laboratory for Cancer Molecular Cell Biology, Life Sciences Institute, Zhejiang University, Hangzhou, China, Department of Orthopedics Surgery, the Second Affiliated Hospital, School of Medicine, Zhejiang University, Hangzhou, China
ORCID iD: 0000-0002-5696-2191

For correspondence: li_shen@zju.edu.cn

Lie Wang
Institute of Immunology and Bone Marrow Transplantation Center, The First Affiliated Hospital, Zhejiang University School of Medicine, Hangzhou, China, Zhejiang University School of Medicine, Hangzhou, China, Liangzhu Laboratory, Zhejiang University Medical Center, Hangzhou, China, Laboratory Animal Center, Zhejiang University, Hangzhou, China, Future Health Laboratory, Innovation Center of Yangtze River Delta, Zhejiang University, Jiaxing, China
ORCID iD: 0000-0001-5094-012X

For correspondence: wanglie@zju.edu.cn

Editors

Reviewing Editor
Shimon Sakaguchi
Osaka University, Osaka, Japan

Senior Editor
Betty Diamond
The Feinstein Institute for Medical Research, Manhasset, United States of America

Reviewer #1 (Public review):

Summary:

This work investigated the role of CXXC-finger protein 1 (CXXC1) in regulatory T cells. CXXC1-bound genomic regions largely overlap with Foxp3-bound regions and regions with H3K4me3 histone modifications in Treg cells. CXXC1 and Foxp3 interact with each other, as shown by co-immunoprecipitation. Mice with Treg-specific CXXC1 knockout (KO) succumb to lymphoproliferative diseases between 3 to 4 weeks of age, similar to Foxp3 KO mice. Although the immune suppression function of CXXC1 KO Treg is comparable to WT Treg in an in vitro assay, these KO Tregs failed to suppress autoimmune diseases such as EAE and colitis in Treg transfer models in vivo. This is partly due to the diminished survival of the KO Tregs after transfer. CXXC1 KO Tregs do not have an altered DNA methylation pattern; instead, they display weakened H3K4me3 modifications within the broad H3K4me3 domains, which contain a set of Treg signature genes. These results suggest that CXXC1 and Foxp3 collaborate to regulate Treg homeostasis and function by promoting Treg signature gene expression through maintaining H3K4me3 modification.

Strengths:

Epigenetic regulation of Treg cells has been a constantly evolving area of research. The current study revealed CXXC1 as a previously unidentified epigenetic regulator of Tregs. The strong phenotype of the knockout mouse supports the critical role CXXC1 plays in Treg cells. Mechanistically, the link between CXXC1 and the maintenance of broad H3K4me3 domains is also a novel finding.

Weaknesses:

The authors addressed the reviewer's critiques fully in the revised manuscript.

https://doi.org/10.7554/eLife.103417.2.sa3

Reviewer #2 (Public review):

FOXP3 has been known to form diverse complexes with different transcription factors and enzymes responsible for epigenetic modifications, but how extracellular signals timely regulate FOXP3 complex dynamics remains to be fully understood. Histone H3K4 tri-methylation (H3K4me3) and CXXC finger protein 1 (CXXC1), which is required to regulate H3K4me3, also remain to be fully investigated in Treg cells. Here, Meng et al. performed a comprehensive analysis of H3K4me3 CUT&Tag assay on Treg cells and a comparison of the dataset with the FOXP3 ChIP-seq dataset revealed that FOXP3 could facilitate the regulation of target genes by promoting H3K4me3 deposition. Moreover, CXXC1-FOXP3 interaction is required for this regulation. They found that specific knockdown of Cxxc1 in Treg leads to spontaneous severe multi-organ inflammation in mice and that Cxxc1-deficient Treg exhibits enhanced activation and impaired suppression activity. In addition, they have also found that CXXC1 shares several binding sites with FOXP3 especially on Treg signature gene loci, which are necessary for maintaining homeostasis and identity of Treg cells.

Comments on revisions:

The authors have fully addressed the reviewers' comments and questions.

https://doi.org/10.7554/eLife.103417.2.sa2

Reviewer #3 (Public review):

In the report entitled "CXXC-finger protein 1 associates with FOXP3 to stabilize homeostasis and suppressive functions of regulatory T cells", the authors demonstrated that Cxxc1-

deletion in Treg cells leads to the development of severe inflammatory disease with impaired suppressive function. Mechanistically, CXXC1 interacts with Foxp3 and regulates the expression of key Treg signature genes by modulating H3K4me3 deposition. Their findings are interesting and significant.

Comments on revisions:

In the revised manuscript, the authors have responded well to all the concerns reviewers raised. The manuscript has further improved.

https://doi.org/10.7554/eLife.103417.2.sa1

Author response:

The following is the authors' response to the original reviews.

> ***Reviewer #1 (Public review):***
>
> *Summary:*
>
> *This work investigated the role of CXXC-finger protein 1 (CXXC1) in regulatory T cells. CXXC1-bound genomic regions largely overlap with Foxp3-bound regions and regions with H3K4me3 histone modifications in Treg cells. CXXC1 and Foxp3 interact with each other, as shown by co-immunoprecipitation. Mice with Treg-specific CXXC1 knockout (KO) succumb to lymphoproliferative diseases between 3 to 4 weeks of age, similar to Foxp3 KO mice. Although the immune suppression function of CXXC1 KO Treg is comparable to WT Treg in an in vitro assay, these KO Tregs failed to suppress autoimmune diseases such as EAE and colitis in Treg transfer models in vivo. This is partly due to the diminished survival of the KO Tregs after transfer. CXXC1 KO Tregs do not have an altered DNA methylation pattern; instead, they display weakened H3K4me3 modifications within the broad H3K4me3 domains, which contain a set of Treg signature genes. These results suggest that CXXC1 and Foxp3 collaborate to regulate Treg homeostasis and function by promoting Treg signature gene expression through maintaining H3K4me3 modification.*
>
> *Strengths:*
>
> *Epigenetic regulation of Treg cells has been a constantly evolving area of research. The current study revealed CXXC1 as a previously unidentified epigenetic regulator of Tregs. The strong phenotype of the knockout mouse supports the critical role CXXC1 plays in Treg cells. Mechanistically, the link between CXXC1 and the maintenance of broad H3K4me3 domains is also a novel finding.*
>
> *Weaknesses:*
>
> *(1) It is not clear why the authors chose to compare H3K4me3 and H3K27me3 enriched genomic regions. There are other histone modifications associated with transcription activation or repression. Please provide justification.*

Thank you for highlighting this important point. We chose to focus on H3K4me3 and H3K27me3 enriched genomic regions because these histone modifications are well-characterized markers of transcriptional activation and repression, respectively. H3K4me3 is predominantly associated with active promoters, while H3K27me3 marks repressed chromatin states, particularly in the context of gene regulation at promoters. This duality provides a robust framework for investigating the balance between transcriptional activation and repression in Treg cells. While histone acetylation, such as H3K27ac, is linked to

enhancer activity and transcriptional elongation, our focus was on promoter-level regulation, where H3K4me3 and H3K27me3 are most relevant. Although other histone modifications could provide additional insights, we chose to focus on these two to maintain clarity and feasibility in our analysis. We have revised the text accordingly; please refer to Page 18, lines 353-356.

> *(2) It is not clear what separates Clusters 1 and 3 in Figure 1C. It seems they share the same features.*

We apologize for not clarifying these clusters clearly. Cluster 1 and 3 are both H3K4me3 only group, with H3K4me3 enrichment and gene expression levels being higher in Cluster 1. At first, we divided the promoters into four categories because we wanted to try to classify them into four categories: H3K4me3 only, H3K27me3 only, H3K4me3-H3K27me3 co-occupied, and None. However, in actual classification, we could not distinguish H3K4me3-H3K27me3 co-occupied group. Instead, we had two categories of H3K4me3 only, with cluster 1 having a higher enrichment level for H3K4me3 and gene expression levels.

> *(3) The claim, "These observations support the hypothesis that FOXP3 primarily functions as an activator by promoting H3K4me3 deposition in Treg cells." (line 344), seems to be a bit of an overstatement. Foxp3 certainly can promote transcription in ways other than promoting H3K3me3 deposition, and it also can repress gene transcription without affecting H3K27me3 deposition. Therefore, it is not justified to claim that promoting H3K4me3 deposition is Foxp3's primary function.*

Thank you for your insightful feedback. We agree that the statement in line 344 may have overstated the role of FOXP3 in promoting H3K4me3 deposition as its primary function. As you pointed out, FOXP3 is indeed a multifaceted transcription factor that regulates gene expression through various mechanisms. It can promote transcription independent of H3K4me3 deposition, as well as repress transcription without directly influencing H3K27me3 levels.

To more accurately reflect the broader regulatory functions of FOXP3, we have revised the manuscript. The updated text (Page 19, lines 385-388) now reads:

"These findings collectively support the conclusion that FOXP3 contributes to transcriptional activation in Treg cells by promoting H3K4me3 deposition at target loci, while also regulating gene expression directly or indirectly through other epigenetic modifications.

> *(4) For the in vitro suppression assay in Figure S4C, and the Treg transfer EAE and colitis experiments in Figure 4, the Tregs should be isolated from Cxxc1 fl/fl x Foxp3 cre/wt female heterozygous mice instead of Cxxc1 fl/fl x Foxp3 cre/cre (or cre/Y) mice. Tregs from the homozygous KO mice are already activated by the lymphoproliferative environment and could have vastly different gene expression patterns and homeostatic features compared to resting Tregs. Therefore, it's not a fair comparison between these activated KO Tregs and resting WT Tregs.*

Thank you for raising this insightful point regarding the potential activation status of Treg cells in homozygous knockout mice. To address this concern, we performed additional experiments using Treg cells isolated from *Foxp3*$^{Cre/+}$*Cxxc1*$^{fl/fl}$ (hereafter referred to as “het-KO”) female mice and their littermate controls, *Foxp3*$^{Cre/+}$*Cxxc1*$^{fl/+}$ (referred to as “het-WT”) mice.

The results of these new experiments are now included in the manuscript (Page25, lines 507–509, Figure 6E and Figure S6A-E):

(1) In the in vitro suppression assay, Treg cells from het-KO mice exhibited reduced suppressive function compared to het-WT Treg cells. This finding underscores the intrinsic defect in Treg cells suppressive capacity attributable to the loss of one *Cxxc1* allele.

(2) In the experimental autoimmune encephalomyelitis (EAE) model, Treg cells isolated from het-KO mice also demonstrated impaired suppressive function.

> *(5) The manuscript didn't provide a potential mechanism for how CXXC1 strengthens broad H3K4me3-modified genomic regions. The authors should perform Foxp3 ChIP-seq or Cut-n-Taq with WT and Cxxc1 cKO Tregs to determine whether CXXC1 deletion changes Foxp3's binding pattern in Treg cells.*

Thank you for raising this important point. To address your suggestion, we performed CUT&Tag experiments and found that *Cxxc1* deletion does not alter FOXP3 binding patterns in Treg cells. Most FOXP3-bound regions in WT Treg cells were similarly enriched in KO Treg cells, indicating that *Cxxc1* deficiency does not impair FOXP3's DNA-binding ability. These results have been added to the revised manuscript (Page 28, lines 567-575, Figure S8A-B) and are further discussed in the Discussion (Pages 28-29, lines 581-587).

> ***Reviewer #2 (Public review):***
>
> *FOXP3 has been known to form diverse complexes with different transcription factors and enzymes responsible for epigenetic modifications, but how extracellular signals timely regulate FOXP3 complex dynamics remains to be fully understood. Histone H3K4 tri-methylation (H3K4me3) and CXXC finger protein 1 (CXXC1), which is required to regulate H3K4me3, also remain to be fully investigated in Treg cells. Here, Meng et al. performed a comprehensive analysis of H3K4me3 CUT&Tag assay on Treg cells and a comparison of the dataset with the FOXP3 ChIP-seq dataset revealed that FOXP3 could facilitate the regulation of target genes by promoting H3K4me3 deposition.*
>
> *Moreover, CXXC1-FOXP3 interaction is required for this regulation. They found that specific knockdown of Cxxc1 in Treg leads to spontaneous severe multi-organ inflammation in mice and that Cxxc1-deficient Treg exhibits enhanced activation and impaired suppression activity. In addition, they have also found that CXXC1 shares several binding sites with FOXP3 especially on Treg signature gene loci, which are necessary for maintaining homeostasis and identity of Treg cells.*
>
> *The findings of the current study are pretty intriguing, and it would be great if the authors could fully address the following comments to support these interesting findings.*
>
> *Major points:*
>
> *(1) There is insufficient evidence in the first part of the Results to support the conclusion that "FOXP3 functions as an activator by promoting H3K4Me3 deposition in Treg cells". The authors should compare the results for H3K4Me3 in FOXP3-negative conventional T cells to demonstrate that at these promoter loci, FOXP3 promotes H3K4Me3 deposition.*

Thank you for this insightful comment. We have already performed additional experiments comparing H3K4Me3 levels between FOXP3-positive Treg cells and FOXP3-negative conventional T cells (Tconv). Please refer to Pages 18, lines 361-368, and Figure 1C and Figure S1C for the results. Our results show that H3K4Me3 abundance is higher at many Treg-specific gene loci in Treg cells compared to Tconv cells. This supports our conclusion that FOXP3 promotes H3K4Me3 deposition at these loci.

> *(2) In Figure 3 F&G, the activation status and IFNγ production should be analyzed in Treg cells and Tconv cells separately rather than in total CD4+ T cells. Moreover, are there changes in autoantibodies and IgG and IgE levels in the serum of cKO mice?*

Thank you for your valuable suggestions. In response to your comment, we reanalyzed the data in Figures 3F and 3G to assess the activation status and IFN-γ production in Tconv cells. The updated analysis revealed that *Cxxc1* deletion in Treg cells leads to increased activation and IFN-γ production in Tconv cells. Additionally, we corrected the analysis of IL-17A and IL-4 expression, which were upregulated in Tconv cells. These updated results are now included in the revised manuscript (Page 21, lines 429-431, Figure 3I and Figure S3E-F).

Additionally, we examined autoantibodies and immunoglobulin levels in the serum of *Cxxc1* cKO mice. Our data show a significant increase in serum IgG levels, accompanied by elevated IgG autoantibodies, indicating heightened autoimmune responses. In contrast, serum IgE levels remained largely unchanged. The results are detailed in the revised manuscript (Page 21, lines 421-423, Figure 3E and Figure S3B).

> *(3) Why did Cxxc1-deficient Treg cells not show impaired suppression than WT Treg during in vitro suppression assay, despite the reduced expression of Treg cell suppression assay -associated markers at the transcriptional level demonstrated in both scRNA-seq and bulk RNA-seq?*

Thank you for your thoughtful comment. The absence of impaired suppression in *Cxxc1*-deficient Treg cells from homozygous knockout (KO) mice during the in vitro suppression assay, despite the reduced expression of Treg-associated markers at the transcriptional level (as demonstrated by scRNA-seq), can likely be explained by the activated state of these Treg cells. In homozygous KO mice, Treg cells are already activated due to the lymphoproliferative environment, resulting in gene expression patterns that differ from those of resting Treg cells. This pre-activation may obscure the effect of *Cxxc1* deletion on their suppressive function in vitro.

To address this limitation, we used heterozygous $Foxp3^{Cre/+}Cxxc1^{fl/fl}$ (het-KO) female mice, along with their littermate controls, $Foxp3^{Cre/+}Cxxc1^{fl/+}$ (het-WT) mice. In these heterozygous mice, we observed an impairment in Treg cell suppressive function in vitro, which was accompanied by the downregulation of several key Treg-associated genes, as confirmed by RNA-Seq analysis.

These updated findings, based on the use of het-KO mice, are now incorporated into the revised manuscript (Page 25, lines 507–509, Figure 6E).

> *(4) Is there a disease in which Cxxc1 is expressed at low levels or absent in Treg cells? Is the same immunodeficiency phenotype present in patients as in mice?*

This is indeed a very meaningful and intriguing question, and we are equally interested in understanding whether low or absent *Cxxc1* expression in Treg cells is associated with any human diseases. However, despite an extensive review of the literature and available data, we found no reports linking *Cxxc1* deficiency in Treg cells to immunodeficiency phenotypes in patients comparable to those observed in mice.

> ***Reviewer #3 (Public review):***
>
> *In the report entitled "CXXC-finger protein 1 associates with FOXP3 to stabilize homeostasis and suppressive functions of regulatory T cells", the authors demonstrated that Cxxc1-deletion in Treg cells leads to the development of severe inflammatory disease*

> *with impaired suppressive function. Mechanistically, CXXC1 interacts with Foxp3 and regulates the expression of key Treg signature genes by modulating H3K4me3 deposition. Their findings are interesting and significant. However, there are several concerns regarding their analysis and conclusions.*
>
> *Major concerns:*
>
> *(1) Despite cKO mice showing an increase in Treg cells in the lymph nodes and Cxxc1-deficient Treg cells having normal suppressive function, the majority of cKO mice died within a month. What causes cKO mice to die from severe inflammation?*
>
> *Considering the results of Figures 4 and 5, a decrease in the Treg cell population due to their reduced proliferative capacity may be one of the causes. It would be informative to analyze the population of tissue Treg cells.*

Thank you for your insightful observation regarding the mortality of cKO mice despite increased Treg cells in lymph nodes and the normal suppressive function of *Cxxc1*-deficient Treg cells.

As suggested, we hypothesized that the reduction of tissue-resident Treg cells could be a key factor. Additional experiments revealed a significant decrease in Treg cell populations in the small intestine lamina propria (LPL), liver, and lung of cKO mice. These findings highlight the critical role of tissue-resident Treg cells in preventing systemic inflammation.

This reduction aligns with Figures 4 and 5, which demonstrate impaired proliferation and survival of *Cxxc1*-deficient Treg cells. Together, these defects lead to insufficient Treg populations in peripheral tissues, escalating localized inflammation into systemic immune dysregulation and early mortality.

These additional results have been incorporated into the revised manuscript (Page21, lines 424-427, Figure 3G and Figure S3C).

> *(2) In Figure 5B, scRNA-seq analysis indicated that the Mki67+ Treg subset is comparable between WT and Cxxc1-deficient Treg cells. On the other hand, FACS analysis demonstrated that Cxxc1-deficient Treg shows less Ki-67 expression compared to WT in Figure 5I. The authors should explain this discrepancy.*

Thank you for pointing out the apparent discrepancy between the scRNA-seq and FACS analyses regarding Ki-67 expression in *Cxxc1*-deficient Treg cells.

In Figure 5B, the scRNA-seq analysis identified the Mki67+ Treg subset as comparable between WT and *Cxxc1*-deficient Treg cells. This finding reflects the overall proportion of cells expressing Mki67 transcripts within the Treg population. In contrast, the FACS analysis in Figure 5I specifically measures Ki-67 protein levels, revealing reduced expression in *Cxxc1*-deficient Treg cells compared to WT.

To resolve this discrepancy, we performed additional analyses of the scRNA-seq data to directly compare the expression levels of Mki67 mRNA between WT and *Cxxc1*-deficient Treg cells. The results revealed a consistent reduction in Mki67 transcript levels in Cxxc1-deficient Treg cells, aligning with the reduced Ki-67 protein levels observed by FACS.

These new analyses have been included in the revised manuscript (Author response image 1) to clarify this point and demonstrate consistency between the scRNA-seq and FACS data.

Author response image 1.

Violin plots displaying the expression levels of Mki67 in T_{reg} cells from *Foxp3*^{cre} and *Foxp3*^{cre}*Cxxc1*$^{fl/fl}$ mice.

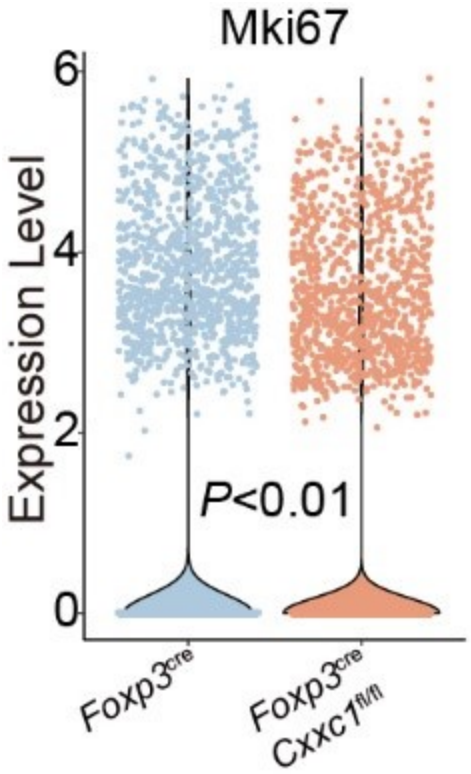

> *In addition, the authors concluded on line 441 that CXXC1 plays a crucial role in maintaining Treg cell stability. However, there appears to be no data on Treg stability. Which data represent the Treg stability?*

Thank you for your valuable comment. We agree that our wording in line 441 may have been too conclusive. Our data focus on the impact of *Cxxc1* deficiency on Treg cell homeostasis and transcriptional regulation, rather than directly measuring Treg cell stability. Specifically, the downregulation of Treg-specific suppressive genes and upregulation of pro-inflammatory markers suggest a shift in Treg cell function, which points to disrupted homeostasis rather than stability.

We have revised the manuscript to clarify that CXXC1 plays a crucial role in maintaining Treg cell function and homeostasis, rather than stability (Page 24, lines 489-491).

> *(3) The authors found that Cxxc1-deficient Treg cells exhibit weaker H3K4me3 signals compared to WT in Figure 7. This result suggests that Cxxc1 regulates H3K4me3 modification via H3K4 methyltransferases in Treg cells. The authors should clarify which H3K4 methyltransferases contribute to the modulation of H3K4me3 deposition by Cxxc1 in Treg cells.*

We appreciate the reviewer's insightful comment regarding the role of H3K4 methyltransferases in regulating H3K4me3 deposition by CXXC1 in Treg cells.

CXXC1 has been reported to function as a non-catalytic component of the Set1/COMPASS complex, which includes the H3K4 methyltransferases SETD1A and SETD1B—key enzymes responsible for H3K4 trimethylation(1-4). Based on these findings, we propose that CXXC1 modulates H3K4me3 levels in Treg cells by interacting with and stabilizing the activity of the Set1/COMPASS complex.

These revisions are further discussed in the Discussion (Page 30-31, lines 624-632).

> *Furthermore, it would be important to investigate whether Cxxc1-deletion alters Foxp3 binding to target genes.*

Thank you for raising this important point. To address your suggestion, we performed CUT&Tag experiments and found that *Cxxc1* deletion does not alter FOXP3 binding patterns in Treg cells. Most FOXP3-bound regions in WT Treg cells were similarly enriched in KO Treg cells, indicating that *Cxxc1* deficiency does not impair FOXP3's DNA-binding ability. These results have been added to the revised manuscript (Page 28, lines 567-575, Figure S8A-B) and are further discussed in the Discussion (Pages 28-29, lines 581-587).

> *(4) In Figure 7, the authors concluded that CXXC1 promotes Treg cell homeostasis and function by preserving the H3K4me3 modification since Cxxc1-deficient Treg cells show lower H3K4me3 densities at the key Treg signature genes. Are these Cxxc1-deficient Treg cells derived from mosaic mice? If Cxxc1-deficient Treg cells are derived from cKO mice, the gene expression and H3K4me3 modification status are inconsistent because scRNA-seq analysis indicated that expression of these Treg signature genes was increased in Cxxc1-deficient Treg cells compared to WT (Figure 5F and G).*

Thank you for your insightful comment. To clarify, the *Cxxc1*-deficient Treg cells analyzed for H3K4me3 modifications in Figure 7 were derived from *Cxxc1* conditional knockout (cKO) mice, not mosaic mice.

Regarding the apparent inconsistency between reduced H3K4me3 levels and the increased expression of Treg signature genes observed in scRNA-seq analysis (Figure 5F and G), we believe this discrepancy can be attributed to distinct mechanisms regulating gene expression. H3K4me3 is an epigenetic mark that facilitates chromatin accessibility and transcriptional regulation, reflecting upstream chromatin dynamics. However, gene expression levels are influenced by a combination of factors, including transcriptional activators, downstream compensatory mechanisms, and the inflammatory environment in cKO mice.

The upregulation of Treg signature genes in scRNA-seq data likely reflects an activated or pro-inflammatory state of *Cxxc1*-deficient Treg cells in response to systemic inflammation, as previously described in the manuscript. This contrasts with the intrinsic reduction in H3K4me3 levels at these loci, indicating a loss of epigenetic regulation by CXXC1.

To further support this interpretation, RNA-seq analysis of Treg cells from *Foxp3*$^{Cre/+}$ *Cxxc1*$^{fl/fl}$ ("het-KO") and their littermate *Foxp3*$^{Cre/+}$ *Cxxc1*$^{fl/+}$ ("het-WT") female mice (Figure S6C) revealed a significant reduction in key Treg signature genes such as *Icos*, *Ctla4*, *Tnfrsf18*, and *Nt5e* in het-KO Treg cells. These results align with the diminished H3K4me3 modifications observed in cKO Treg cells, further underscoring the role of CXXC1 as an epigenetic regulator.

In summary, while the gene expression changes observed in scRNA-seq may reflect adaptive responses to inflammation, the reduced H3K4me3 modifications directly highlight the critical role of CXXC1 in maintaining the epigenetic landscape essential for Treg cell homeostasis and function.

> ***Recommendations for the authors:***
>
> ***Reviewer #1 (Recommendations for the authors):***
>
> *In Figure 7E, the y-axis scale for H3K4me3 peaks at the Ctla4 locus should be consistent between WT and cKO samples.*

We thank the reviewer for pointing out the inconsistency in the y-axis scale for the H3K4me3 peaks at the *Ctla4* locus in Figure 7E. We have carefully revised the figure to ensure that the y-axis scale is now consistent between the WT and cKO samples.

We appreciate the reviewer's attention to this detail, as it enhances the rigor of the data presentation. Please find the updated Figure 7E in the revised manuscript.

> ***Reviewer #2 (Recommendations for the authors):***
>
> *In lines 455 and 466, the name of Treg signature markers validated by flow cytometry should be written as protein name and capitalized.*

Thank you for pointing this out. We have carefully reviewed lines 455 and 466 and have revised the text to ensure that the Treg signature markers validated by flow cytometry are referred to using their protein names, with proper capitalization.

> ***Reviewer #3 (Recommendations for the authors):***
>
> *(1) On line 431, "Cxxc1-deficient cells" should be Cxxc1-deficient Treg cells".*

We thank the reviewer for highlighting this oversight. On line 431, we have revised "Cxxc1-deficient cells" to "Cxxc1-deficient Treg cells" to provide a more accurate and specific description. We appreciate the reviewer's attention to detail, as this correction improves the precision of our manuscript.

> *(2) In Figure 4H, negative values should be removed from the y-axis.*

Thank you for your observation. We have revised Figure 4H to remove the negative values from the y-axis, as requested. This adjustment ensures a more accurate and meaningful representation of the data.

> *(3) It is better to provide the lists of overlapping genes in Figure 7C.*

Thank you for your suggestion. We agree that providing the lists of overlapping genes in Figure 7C would enhance the clarity and reproducibility of the results. We have now included the gene lists as supplementary information (Supplementary Table 3) accompanying Figure 7C.

(1) Lee, J. H. & Skalnik, D. G. CpG-binding protein (CXXC finger protein 1) is a component of the mammalian set1 histone H3-Lys4 methyltransferase complex, the analogue of the yeast Set1/COMPASS complex. Journal of Biological Chemistry 280, 41725-41731, doi:10.1074/jbc.M508312200 (2005).

(2) Thomson, J. P., Skene, P. J., Selfridge, J., Clouaire, T., Guy, J., Webb, S., Kerr, A. R. W., Deaton, A., Andrews, R., James, K. D., Turner, D. J., Illingworth, R. & Bird, A. CpG islands influence chromatin structure via the CpG-binding protein Cfp1. Nature 464, 1082-U1162, doi:10.1038/nature08924 (2010).

(3) Shilatifard, A. in Annual Review of Biochemistry, Vol 81 Vol. 81 Annual Review of Biochemistry (ed R. D. Kornberg) 65-95 (2012).

(4) Brown, D. A., Di Cerbo, V., Feldmann, A., Ahn, J., Ito, S., Blackledge, N. P., Nakayama, M., McClellan, M., Dimitrova, E., Turberfield, A. H., Long, H. K., King, H. W., Kriaucionis, S., Schermelleh, L., Kutateladze, T. G., Koseki, H. & Klose, R. J. The SET1 Complex Selects Actively Transcribed Target Genes via Multivalent Interaction with CpG Island Chromatin. Cell Reports 20, 2313-2327, doi:10.1016/j.celrep.2017.08.030 (2017).

https://doi.org/10.7554/eLife.103417.2.sa0